Improved Draw Process in Optical Fiber Fabrication

by

Shah M. Musa

Thesis submitted to the Faculty of the

Virginia Polytechnic Institute and State University

in partial fulfillment of the requirements for the degree of

Master of Science

in

Electrical Engineering

APPROVED:

Dr. Kent A. Murphy, Chairman

Dr. Richard O. Claus

Dr. Anbo Wang

November 1994

Blacksburg, Virginia

c.2

Improved Draw Process in Optical Fiber Fabrication

by

Shah M. Musa

Committee chairman: Dr. Kent Murphy

Department of Electrical Engineering

(ABSTRACT)

The performance of an optical fiber depends to a great extent on the conditions of the process being used to draw the fiber from a glass preform. To get fibers with higher strength and lower transmission loss, the parameters of the draw process must be optimized and the geometric uniformity of the fiber must be maintained with high precision. To increase the geometric uniformity of the fiber the on-line fiber diameter measuring accuracy must be improved. The coating concentricity and uniformity also play an important role in fabricating quality fiber. As the fiber drawing speed goes higher and higher, which is the trend of modern fiber fabrication processes, the uniformity of fiber diameter and coating concentricity becomes even tougher to maintain. The main objective of this research has been to understand and develop an optical fiber drawing process that produces fiber with improved dimensional uniformity, higher strength and lower transmission loss. Particular emphasis has been given to the accurate measurement of on-line fiber diameter, which is the first and most important step in obtaining uniform fiber.

ACKNOWLEDGMENTS

I would like to express my gratitude and deepest appreciation to my advisor Dr. Kent A. Murphy, for his enthusiastic encouragement and support to complete this thesis. I would also like to acknowledge the contributions of the members of my advisory committee, Dr. Richard O. Claus and Dr. Anbo Wang. I thank all my friends and teachers of Virginia Tech for providing me an excellent learning environment.

Thanks to Kenneth Lane and Steve Hobeck and all other engineers of Alcatel Cable Systems, Roanoke, Virginia, for giving me the opportunity to work in a very friendly environment of the fiber fabrication group there during the summer of 1993.

Finally, I would like to thank my family, especially my sisters and parents, for their endless support to my graduate studies which made this work possible.

CONTENTS

FIGURES Page number

CHAPTER 1

Introduction

1.1 Background

During the last couple of decades, optical fiber communication systems have enjoyed widespread applications, all over the world, mainly due to its low transmission loss and wide bandwidth, small size and weight, immunity to interference, signal security and low cost [Keiser, 1991]. All these advantages over conventional copper wire systems have been appreciated by using fiber not only in the long haul trunking application including undersea cable, but also in the local subscriber loop. Cable television companies have also recently started using optical fibers for analog video distribution as fiber has more information capacity than the coaxial cable. Optical fiber will also allow them to broadcast digital video channels in the future. The oncoming Information Super Highway will make optical fiber even more widespread, leading ultimately to connect every house with a fiber. Optical fiber is also being used more and more as a sensing and measuring instrument [Dakin and Culshaw, 1988].

All these applications of optical fiber have given a boost to the fiber fabrication industries. It is a challenging job to fabricate fiber that satisfies current stringent specifications. The fiber must have,

a) low transmission loss (0.2 to 0.4 dB/km),

b) high-strength (over 100 kpsi),

c) long length without any break (up to 40 km),

d) minimum diameter variation (less than 1 μm from the nominal value), and

e) high reliability.

Low transmission loss is necessary for high bit rate and long distance optical communications. Fibers must be of high-strength so that they can go through rough handling required in shipping, cabling and installing. Long lengths of fiber without any breaks reduce the need for lossy splices in long-haul optical communications. Minimum diameter variation is important to reduce coupling as well as transmission losses. And high reliability of optical fiber is essential to make a system economically viable.

Even though the most of the equipment and facilities are available from commercial sources, the fiber fabrication process is not yet in complete maturity. To keep up with the competitive market, research and development have become an integrated part of the fiber fabrication process. Also the flexibility of adopting new processes is essential for fiber fabrication industries.

1.2 Purpose of the Research

The main objective of this research has been to understand and develop an optical fiber drawing process that produces fiber with improved dimensional uniformity, higher strength and lower transmission loss. Particular emphasis has been given to the accurate measurement of on-line fiber diameter, which is the first and most important step in obtaining uniform fiber. Among the factors responsible for inaccuracy of on-line fiber diameter measurement are:

a) The inherent inaccuracies of the diameter measuring system: These inaccuracies are listed in the specifications manual of the particular system. Different companies make different types of diameter measuring systems having their own inherent inaccuracies which depend on the

particular technique and structure they have chosen. This inaccuracy is statistical in nature and can not be avoided during the fiber drawing process. It is out of the scope of our research to find out how to improve the inherent inaccuracy of a diameter measuring system.

b) The proper calibration of the diameter measuring system: The quality and stability of the standard with which the system is calibrated affects the fiber diameter measuring accuracy. If the calibrating standard is made using metal, while the diameter we wish to measure is an optical fiber, there may be a significant amount of inaccuracy introduced in the measurement.

c) The proper placement of the fiber, of which the diameter is being measured, with respect to the diameter measuring system: Proper positioning is necessary to improve the measurement accuracy of the fiber diameter. It has been observed, see Chapter 3, that the diameter measured by the diameter measuring system varies with lateral position shift of the fiber with respect to the system. Bends in the preform produce (all preforms have bends, at least microbends) produce lateral shifts causing the fiber to move with respect to the diameter measuring system.

d) The mechanical vibration of the fiber while it is being drawn: Some mechanical vibrations of the optical fiber are inavoidable in the draw process. The nature of these vibrations depends on the characteristics of the motors being used in the drawing process as well as on the coating parameters such as the coating fluid mechanics, the shape of the coating applicator and also on the cooling process of the fiber. These vibrations vary with varying speeds of the motors and may have different effects on the fiber diameter measuring accuracy at different draw speeds. The actual amount of inaccuracies introduced by the vibrations depend on the particular technique used in the measuring system for the fiber diameter measurement. Our research does

not deal with the nature of vibrations of the fiber in the draw process or its effect on the measuring accuracy for any particular diameter measuring system at different speeds, but it analyses the techniqes to achieve high-speed drawing with optimum transmission loss and uniform coating of the fiber. The drawing speed of the fiber is mainly limited by the coating parameters as the type of coating fluid, the coating applicator, the ultra-violet (UV) cure of coating, and also by the fiber cooling process.

Usually the optical fiber fabrication industries use metallic standards to calibrate their diameter measuring systems, which introduce some inaccuracies, or an offset, to the measured diameter. In this research we develop a procedure to make glass standards using optical fiber itself, which gives a better measurement accuracy. We also demonstrate a novel discrete feedback system to the glass preform to keep the fiber always at a lateral fixed position with respect to the diameter measuring system. The feedback is discrete because a continuous feedback increases the vibration of the preform causing the fiber to be even more nonuniform in dimension.

1.3 Overview of the Thesis

The overall draw-process has been investigated in this thesis with particular emphasis on diameter control and measurement. The thesis has been arranged in five chapters. Chapter 1 gives the background and the purpose of the research. Chapter 2 outlines the draw process of the optical fiber including the melting process of the preform and the drawing dependent losses introduced during the melting process. It also describes different heating furnaces used in preform melting and the environment necessary for low-loss high-strength fiber drawing. Chapter 3 discusses different diameter measuring techniques and the ways to improve diameter uniformity of optical fiber. It presents a detailed study of an on-line diameter

measuring system, Anritsu M551A, and develops a procedure of making glass standards for its calibration. It also develops a feedback procedure to place the fiber always at a lateral fixed position, with respect to diameter measuring system, to improve the measuring accuracy of the diameter. Chapter 4 deals with coating of optical fiber. It discusses coating fluids and applicators, UV cure, high-speed coating, and features associated with high-speed coating. It also discusses UV induced losses in optical fiber. Chapter 5 contains the conclusion and suggestion for future research. References are given at the end of Chapter 5.

CHAPTER 2

Drawing Optical Fiber From Preform

2.1 Outline of a Draw System:

The huge demand of low-loss high-strength optical fiber with greater dimensional uniformity has given way to the development of very high-speed draw facilities requiring very sophisticated and precise equipment. The essential components of such a draw facility are glass preform (most high quality optical fibers are drawn from glass preforms rather than from crucibles), preform feed system, melting furnace, fiber diameter measuring system, coating applicator system, coating curing system, a draw servo motor (which pulls the fiber), winding capstan, and a tall tower (7-12 m) which holds the preform at the top [DiMarcello et al., 1985]. Fig. 2.1 shows a schematic diagram of a draw facility.

A modern draw process is highly automated with computerized control of the process parameters. An operator is rarely required except to start and stop drawing and when emergency situations arise. The operator's expertise is required to start the drawing process, which can be quite sophisticated.

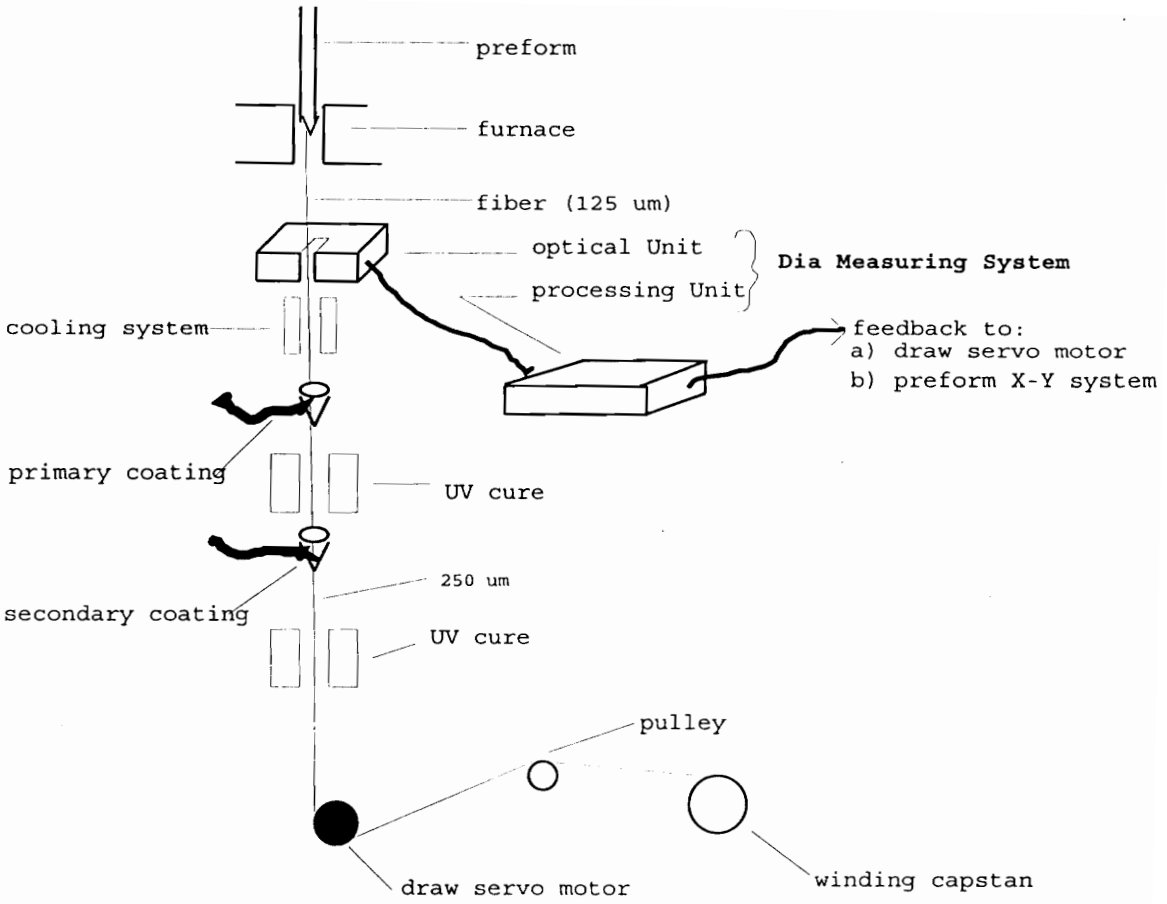

Fig. 2.1 Schematic of a draw system.

2.2 Heating Furnace

A temperature of about 2000°C is required to melt a preform and draw fiber. Different types of furnaces have evolved and are being used for this purpose [Jaeger et al., 1979, book1]. Among these types are oxy-hydrogen burner, electrical resistance or induction furnace, and CO_2 laser furnace [Cocito et al., 1981].

Oxy-hydrogen burners, though cheap and easy to use, are not suitable to fabricate fibers having transmission loss lower than 2dB/km [Cocito et al., 1981], mainly because of introduction of hydroxyl groups during the melting process. Another disadvantage of oxy-hydrogen burners is the imprecise control of furnace temperature caused by the unstable flame which produces fiber with nonuniform diameter.

Resistance furnaces are very popular due to the ability to better control of temperature and uniform heating profile. Usually the resistive material is a pure graphite element. Fig. 2.2(a) shows a schematic of such a furnace. The iris diaphragms obstruct the atmospheric oxygen from entering in the furnace, while a controlled flow of inert gas, such as Argon, is maintained inside the furnace which prevents any oxidation even at very high temperatures. It is also possible to control the fiber diameter by regulating the gas flow [Imoto et al., 1977]. Usually a huge amount of current is required (over 100 A) for these furnaces. The graphite resistance furnaces have very short response times to temperature variations and can reach the operating temperature from room temperature within 5-15 minutes. The contamination of the fiber caused by the graphite dust and the associated impurities can be greatly reduced by using ultrapure graphite, optimizing the gas flow, and cleaning the furnace thoroughly before starting each preform. The graphite needs to be replaced every 2-3 weeks of continuous use.

In induction furnaces the heater is formed by a susceptor heated by rf induction. Usually the susceptor is a cylindrical zirconia or graphite element. The zirconia induction furnaces have excellent control over the heating temperature which can be maintained within ±1°C of the nominal value using a feedback control loop from an optical pyrometer to the rf generator [DiMarcello et al., 1985]. They also have longer life times than resistance furnaces; as long as 3-6 months of continuous usage. They can be operated up to 2500°C in an oxidizing atmosphere, with minimal contamination of the furnace atmosphere, using high-frequency (1-10 MHz) induction. Fig. 2.2(b) shows the schematic of such a zirconia induction furnace. The main disadvantage is that the susceptor can not be coupled directly to the induction field at the start, because the resistivity of zirconia susceptor is too high (over 10^4 ohm/cm) at low temperatures [Cocito et al., 1981]. It must be preheated, by coupling with a carbon rod, up to over 1400°C at which the electrical resistance of the zirconia susceptor becomes sufficiently low allowing the removal of the carbon rod without causing thermal shocks to the susceptor. Thus it takes about 30 minutes to reach the operating temperature. Rapid changes in temperature may cause fractures to the zirconia susceptors. To avoid these problems it is better to keep the furnace always on and at around 1600°C even when it is not being used.

The CO_2 laser heat source can give a cleaner thermal environment. Among the main advantages of using CO_2 laser are [Oehrle, 1979]: (a) minimum contamination of the neck-down region which is essential for low-loss high-strength fibers (b) very easy to start-up and shut-down and (c) fibers can be drawn with elliptical cross sections. A sophisticated system is required to uniformly distribute the laser energy around the melt zone, shown in Fig. 2.3. As shown in the figure the heated zone can actually be very small, which makes it thermally very efficient. But one big problem with CO_2 laser heat source is that it can not be used in high-speed drawing and for large (>10 mm) size preforms. The energy of CO_2 laser is at ~10 μm wavelength at which glass is opaque. So the incident energy remains essentially within

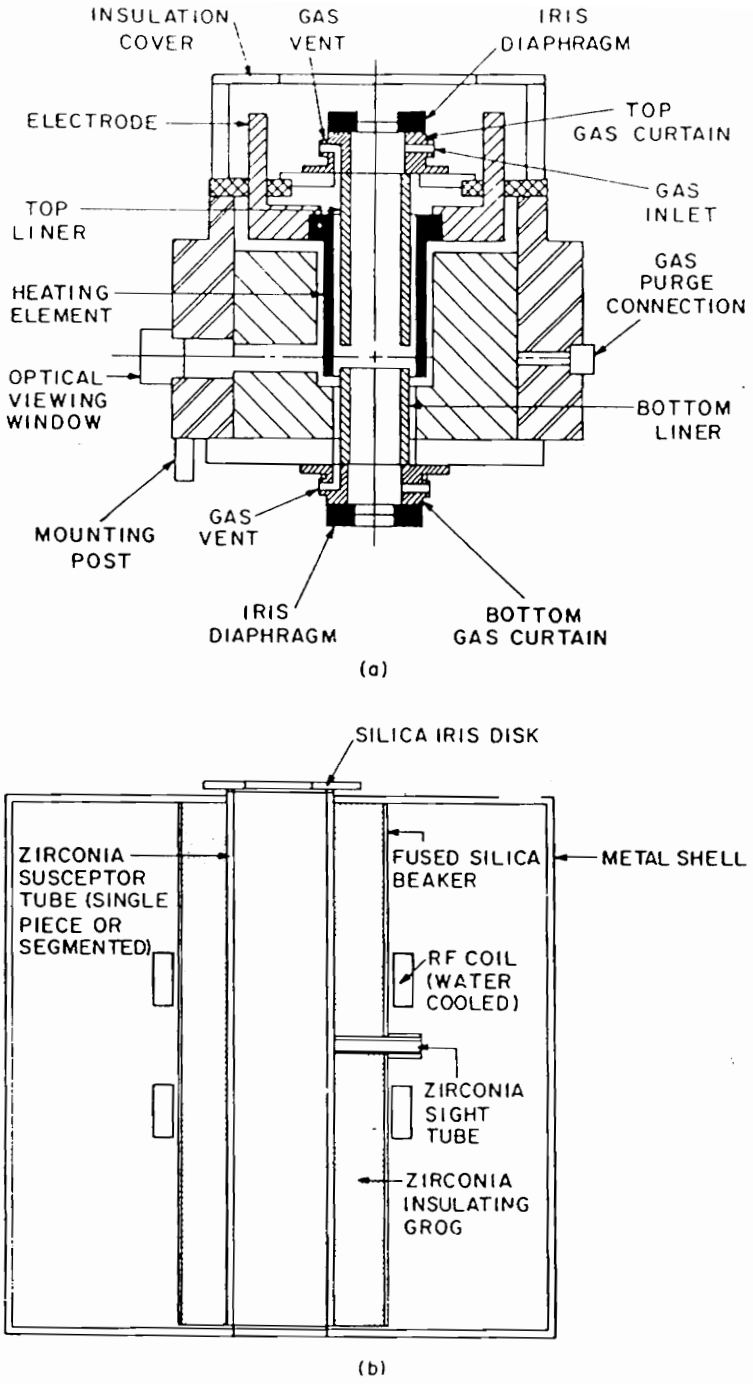

Fig. 2.2 (a) Schematic of a graphite resistance furnace and (b) Schematic of an inductively heated zirconia furnace [DiMarcello et al., 1985].

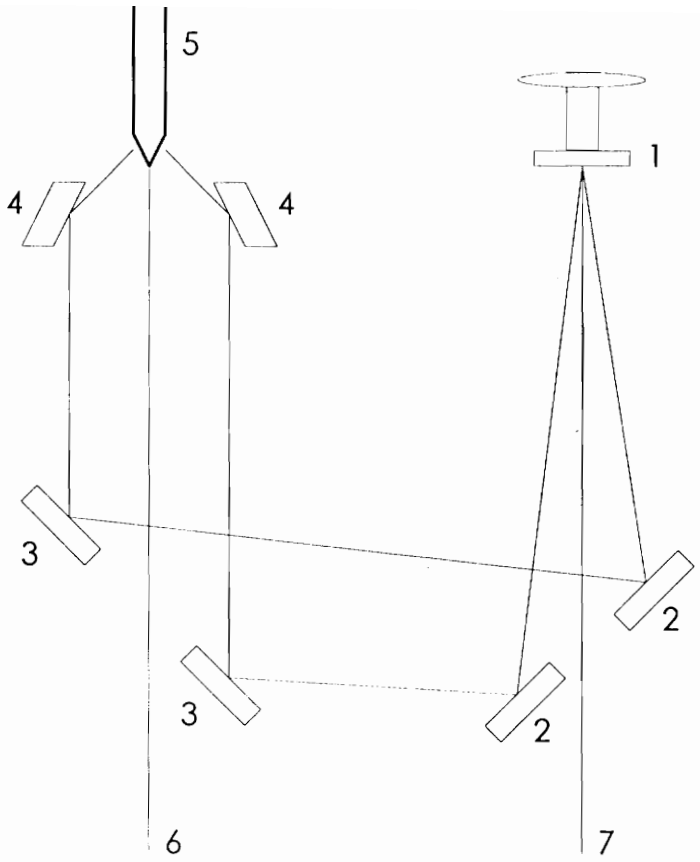

Fig. 2.3 Schematic diagram of a laser furnace: 1) rotating disc mirror; 2-3) mirrors; 4) focus mirror; 5) preform; 6) optical fiber; 7) CO_2 laser beam [after Montierth, 1977].

a thin surface layer causing a high radial temperature gradient which prohibits high-speed drawing of fiber. Increased laser power does not result in an increased speed, but can cause surface vaporization. A lag in the surface-to-center temperature can be as big as 700 °C and with conventional lasers a draw speed greater than 1 m/s is difficult to achieve [Homsy and Walker, 1979].

2.3 The Neck-Down Region

In most cases fiber is produced from a glass preform which is passed through a furnace where it is heated and then drawn along the axial direction. The diameter of the drawn fiber depends upon the diameter of the preform, the rate at which the preform is fed into the furnace, and the rate at which the fiber is pulled by the capstan. As the preform passes through the heating zone it experiences a change in temperature profiled by the furnace. This phenomena along with the drawing tension of the fiber gives way to a "neck-down" shape in the heating zone [Paek and Runk, 1978]. Fig. 2.4 shows the schematic of such a neck-down region. The shape and the behavior of the neck-down region has a great impact on the diameter uniformity, the strength, and the transmission loss of the fiber. In the Fig. 2.4 the neck-down region starts at $z=0$ and ends at $z=L$. The boundary conditions for the axial velocity, V_z, in the neck-down region are,

$$V_z = V_1 \qquad \text{at} \qquad z=0 \ , \tag{2.1}$$

$$V_z = V_2 \qquad \text{at} \qquad z=L \ , \tag{2.2}$$

where V_1 is the preform feed rate and V_2 is the fiber drawing rate. The velocity in the radial direction, V_r, in the neck-down region can be given as [Paek and Runk, 1978],

$$V_r = -\frac{1}{2} r \frac{\partial}{\partial z} V_z . \tag{2.3}$$

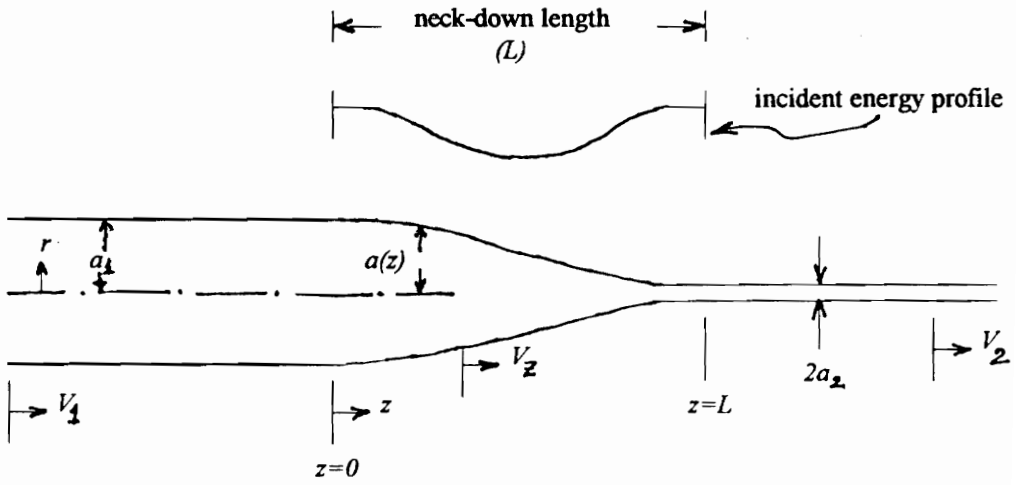

Fig. 2.4 Neck-down region and its axis geometry.

It is obvious from Eq. (2.3) that there is no radial flow at the axis of the preform, at r=0, as expected. Also there is no radial flow beyond the neck-down region, as the axial velocities are independent of z at these regions.

The axial velocity in the neck-down region can be found once the neck-down profile, *a(z)*, is known. The neck-down profile is found by applying the mass conservation,

$$a^2(z)V_z = a_1{}^2V_1, \tag{2.4}$$

where *a(z)* and a_1 is as shown in Fig. 2.4. Eq. (2.4) is only true for simple one dimensional extensional flow which generally applies for fibers drawn from preforms as well as fibers drawn from crucibles [Geyling and Homsy, 1980].

The shape of the neck-down profile, *a(z)*, is governed by the drawing speed V_2, the drawing tension, and the profile of the temperature of the furnace. An empirical formula capable of fitting the neck-down profile of laser-drawn preforms has been given as [Homsy and Walker, 1979],

$$a(z) = \frac{a_1 + a_2}{2} - \frac{a_1 - a_2}{\pi}\tan^{-1}\left\{\frac{z - z_1}{\delta_a}\right\}, \tag{2.5}$$

where z_1 can be the distance of the point of maximum laser intensity, measured axially from the start of the neck-down region, and δ_a is the profile thickness which depends on the width of laser focus.

As the fiber comes out of the heating zone, it starts cooling by radiation and convection to the environment. Applying mass conservation, the final diameter of the fiber, a_2, can be found as,

$$a_2 = a_1\left(\frac{V_1}{V_2}\right)^{1/2}. \tag{2.6}$$

2.4 Drawing Induced Imperfections

The conditions under which the fiber is drawn from a preform can greatly affect its performance. The interplay of temperature, tension and speed exerted on fiber during the draw process is very important and must be understood well to achieve better quality fiber. Imperfections are added to the fiber during the melting and necking process as it undergoes very high temperature, stress, strain and viscosity changes. Losses could be minimized if the mechanisms that cause them can be traced out. We discuss some imperfections introduced during the drawing process and try to identify the factors that are responsible for those imperfections.

a) Drawing induced losses in pure silica fibers: A loss band has been observed in unclad fibers made from vitreous silica of low OH content having a peak around 630 nm and it has been shown that this loss is introduced into the fiber during the drawing process [Kaiser, 1974]. The reason of this loss band has been attributed to the rupture of silicon-oxygen bond (Si-O-Si) which occurs at high temperature when the glass structure experiences very high stresses and structural deformations. Besides the absorption peak, a resonance fluorescence was also observed at 630-nm contributing about 15-20% of the total excess loss peak at this wavelength. This loss is absent in fibers drawn from large preforms, while the intensity of the loss increases with decreasing fiber diameter. The 630-nm loss can also be observed as a coloration when the fibers are being drawn. This loss is of particular importance when a GaP light-emitting-diode is used as a light source for signal transmission, because it emits light in a band centered near 700 nm and the tail of the 630-m loss can affect it significantly.

The 630-nm loss band of silica fiber can be reduced and even eliminated by annealing the drawn fiber at elevated temperatures or exposing it to the room temperature for weeks. But annealing the fiber can cause a higher OH content in the fiber, increasing the OH peak centered at 945 nm. The high-OH-content silica fibers exhibit lower 630-nm losses after the drawing process [Kaiser, 1974].

b) Absorption losses in singlemode fibers with germanium doped cores: Absorption losses are introduced into fiber drawn from a preform with germanium doped core drawn at high temperatures [Ainslie et al., 1981]. This loss increases when either the fiber drawing temperature or the germanium concentration or both of them are increased. This phenomena is of particular importance for dispersion shifted fiber in which the wavelength of the minimum dispersion is shifted from 1.31 μm to 1.55 μm to take advantage of lower loss at 1.55 μm. In order to achieve this dispersion shift in the fiber a smaller core diameter and a higher refractive index difference (Δ n) between core and cladding are necessary. But increasing the core germanium concentration, to get higher refractive index differences, can introduce a high amount of excess loss at high drawing temperatures. This loss is visible at all wavelengths, decreasing slowly with increasing wavelength. The reason for this loss has been attributed to the UV radiation of the furnace which introduces bonding defects. Even though it may seem that the UV radiation in the furnace is too low for any significant effect on the fiber, the exposure time for the glass in the furnace is very long.

The loss introduced in fibers from germanium doped core preforms can be reduced significantly by reducing the drawing temperature. The dispersion shift can also be achieved by depressing the cladding index with fluorine, as opposed to increasing the core germanium concentration.

c) Absorption losses in phosphorus-doped fibers: A coloration loss having a peak centered around 530 nm has been observed in phosphorus-doped low-OH-content optical fiber [Yamauchi et al., 1977]. The loss intensity is almost independent of the furnace temperature but varies with the amount of OH content. Fibers drawn from high-OH-content preforms have very reduced amount of loss in the band. Fig. 2.5 shows the typical spectral losses of phosphorus-doped low-OH-content fibers. The loss has been attributed to the defects of P-O bonds occurring at the drawing temperature.

The loss introduced in phosphorus-doped fibers can easily be reduced by annealing the fiber at elevated or room temperature as Fig. 2.5 indicates. Fibers with high-OH-content presents more rapid reduction of coloration under the annealing process than the fibers with low-OH-content. The coloration is also reduced during the cabling process, as it undergoes various heating processes in cabling.

d) Drawing induced stresses in optical fiber: Because the core and the cladding of a preform are not made out of the exact same materials, they have different coefficients of thermal expansions. So, when the preform is heated in the furnace the core and the cladding experience different amounts of expansion per unit volume. At the neck-down region and after, the cladding starts to solidify first as it can radiate energy faster than the core. The applied tension, at the point when the core is still in flux, gives a tensile stress only at the outer part of the fiber which is under the transition temperature [Brehm et al., 1988]. This unequal tensile stress and different cooling environment and time for the core and the cladding of the fiber can give way to a highly stressed region at the core-cladding interface. This ring of high stress can generate some defects in the fiber which may absorb particular wavelength bands [Ainslie et al., 1982]. The larger the core-

cladding ratio, the more susceptible the fiber is to develop this residual stress during the drawing process.

e) Effect of drawing tension on fiber properties: The tension applied during the drawing process has a very significant impact on fiber strength as well as its transmission loss. A lower drawing tension is favorable to achieve high-strength fibers, while a higher drawing tension is necessary to achieve low-loss transmission fibers [Oh et al., 1983]. At steady state, the drawing tension, F, is related to absolute temperature as,

$$\ln F = [\, A + B/T \,] \ , \tag{2.7}$$

where it is assumed that both temperature and velocity distributions are unidimensional and where A and B are constants for surface tension and viscous flow, respectively [Oh et al., 1983].

Fig. 2.6 shows relationship between drawing speed and drawing tension with furnace temperature as a parameter. The curves are shown for preform diameter of 7.5 mm and fiber diameter of 140 μm having feedback control utilizing both gas-flow and drawing speed. To achieve the optimum transmission loss, the tension must be kept within a proper range to reduce the tension induced irregular variations in the core-cladding interface [Imoto and Sumi, 1978].

2.5 Drawing Environment

Fibers may be contaminated by dust particles in the furnace or on the way to the coating applicator when it is exposed to air. This kind of contamination can reduce the fiber strength and increase the optical transmission losses eventually causing the fiber fail to meet stringent specifications. Fig. 2.7

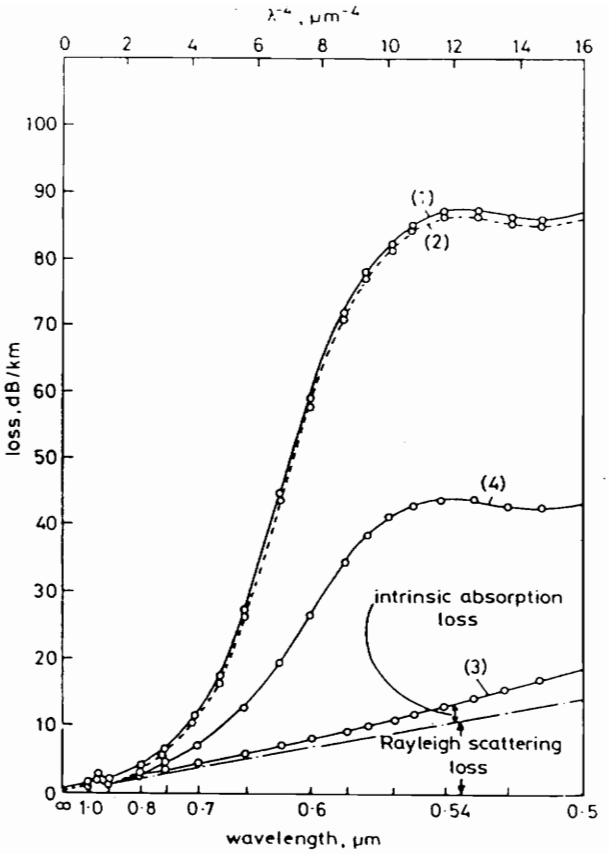

Fig. 2.5 Spectral losses of low-OH content phosphorus-doped silica fiber

(1) Measured immediately after drawing at 2100°C

(2) Measured immediately after drawing at 1900°C

(3) After annealing the fiber of curve 1 at 100°C, 48h

(4) After annealing the fiber of curve 1 at room temperature, 2 months

[Yamauchi et al., 1977].

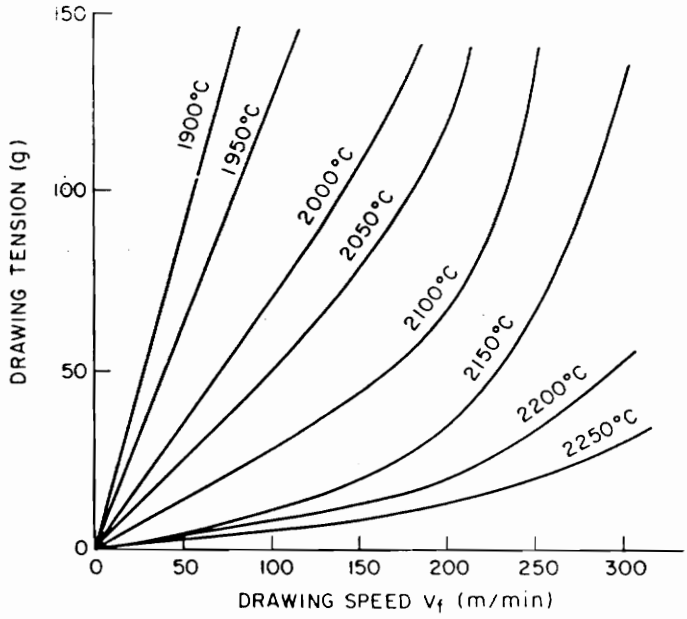

Fig. 2.6 Drawing tension versus drawing speed at various furnace temperatures [Imoto and Sumi, 1978].

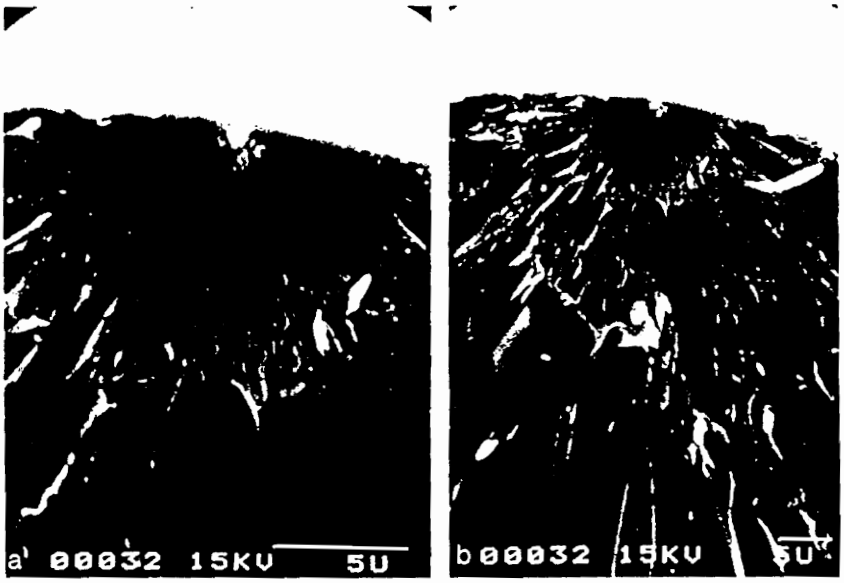

Fig. 2.7 Fracture surface of a fiber that failed due to the contamination with a dust particle: (a) is a magnification of surface (b) [DiMarcello et al., 1985].

shows the fracture surface of a fiber that failed due to contamination with a dust particle. The coating fluid may also be contaminated by dust particles causing a great reduction of the fiber strength. To avoid these problems a very clean filtered air, free of dust particles, is maintained in the drawing room. For example, a class 100 quality air has fewer than 100 particles per cubic foot of air that are 0.5 μm and larger and not more than one particle that is 4.0 μm or larger.

CHAPTER 3

Diameter Measurement and Control

3.1 Controlling the Diameter of Optical Fiber

High performance optical fiber communication systems require very uniform fiber, having diameter variations as small as possible. This requirement is due partly to very tight tolerances in current splice and connector technologies. Splicing may be very difficult for slow long-range variations of the fiber diameter, which is even more critical for singlemode fibers as compared to multimode fibers. In singlemode, the diameter of the core is very small, typically on the order of 10 μm or less, and even a slight misalignment of fibers in a splice can cause a very high transmission loss. Also, it is essential to have very small variations in the fiber diameter to decrease the transmission loss and increase the mechanical strength of the fiber. Rapid short-range variations of the fiber diameter can lead to scattering loss and unpredictable mode-coupling effects [Marcuse, 1974].

There are many factors that may cause fluctuations in diameter of a fiber, including,

a) diameter variations in the preform,

b) bubbles or dust in the preform,

c) bends in the preform,

d) preform feed velocity,

e) gas flow rate of the furnace,

f) temperature stability of the heat source,

g) draw speed of the fiber, and

h) vibrations, both acoustic and mechanical.

Slow varying factors such as bends in the preform cause the long-range fiber diameter variations while the rapidly varying factors such as vibrations of the preform cause the short-range diameter variations.

To control the fiber diameter within a specified limit, typically within ±1 μm of its nominal value, it is necessary to continuously monitor the on-line fiber diameter and apply proper feedback to control various parameters and keep the fiber diameter near the nominal value, as close as possible. There are several strategies in which the feedback system can be applied to control the fiber diameter. Some of the strategies are:

a) feedback to the preform feed rate: The diameter uniformity of an optical fiber can be controlled by applying a feedback to the preform feed rate. When the diameter of the fiber is less than the nominal value, the feed rate of the preform is increased and when the diameter of the fiber is greater than the nominal value, the feed rate of the preform is decreased. This method is very imprecise and usually not used in industries. The diameter of a preform is very large compared to a fiber diameter and a very small change in preform feed rate can cause very high fluctuations in the fiber diameter.

b) feedback to gas flow rate of the furnace: A very quick response in controlling the fiber diameter can be achieved by controlling the gas flow rate of the furnace [Imoto et al., 1977]. In this method an additional flow rate of gas, ΔF, is either added or subtracted from the steady gas flow rate, F, depending on whether the monitored fiber diameter is below or over the nominal

value. ΔF must be kept in a specified range, as an excessively large ΔF generates unmanageable drawing conditions.

c) feedback to fiber drawing speed: The most widely used feedback system applied in industry is feedback to the draw speed to control fiber diameter. In this method the diameter uniformity is maintained by varying the draw speed to compensate for diameter fluctuations while keeping the other factors constant. If the diameter measured is higher than the nominal value, the speed of the draw motor is increased to reduce the fiber diameter and bring it near to the nominal value. Similarly when the monitored diameter is lower than the nominal value, the speed of the draw motor is reduced to increase the fiber diameter and bring it cccloser to the nominal value.

In all the feedback systems, there is a delay between the time at which the fiber is measured and the time the fiber changes diameter in response to the feedback rate change. This delay is because the measurement system is physically positioned some distance below the heat source. By increasing the draw speed, the time-delay defect of measurement can be decreased.

3.2 On-Line Fiber Diameter Measuring Techniques

There are several noncontact techniques which can be applied to measure on-line fiber diameter. The mostly used techniques are discussed below:

a) fiber diameter measurement using forward light scattering: The diameter of a clad fiber can be measured by illuminating it with a light beam perpendicular to the fiber axis and then applying some measurement characteristics to the forward light scattering pattern [Smithgall et al.,

1977]. The pattern makes interference fringes of varying intensity in an angular range of ±(5-90°) around the fiber in the plane perpendicular to its axis. As the diameter changes the number and the spacing of the fringes in a particular measuring angle range also changes. The diameter of the fiber, *2a*, can be measured by counting the number of fringes, *N*, in the scattering angle range and applying the equation [Smithgall et al., 1977],

$$N = \frac{2a}{\lambda}\left\{\left[\sin\frac{\theta_2}{2} + \left(m^2 + 1 - 2m\cos\frac{\theta_2}{2}\right)^{1/2}\right] - \left[\sin\frac{\theta_1}{2} + \left(m^2 + 1 - 2m\cos\frac{\theta_1}{2}\right)^{1/2}\right]\right\}, \quad (3.1)$$

where m is the fiber refractive index, λ is the light wavelength and θ_1 and θ_2 are the bounds of the scattering angle range.

For unclad fibers ~3° is the smallest scattering angle for which the interference fringe pattern can be resolved. The largest scattering angle to get an interference fringe pattern is about 93° [Smithgall et al., 1977]. Thus there is an angle range of about 90° over which the fringes can be counted. Fig 3.1 shows a schematic of a measuring arrangement of forward scattering pattern.

If θ_1 =3° and θ_2 =90° and the refractive index m=1.456, then using equation (3.1), we get,

$$N = 1.25\left(\frac{b}{\lambda}\right) , \quad (3.2)$$

Eq. (3.2) indicates that there are 1.25 fringes for each λ change in fiber diameter and if N is counted only as an integer, the maximum resolution that can be achieved is 0.8λ . As a result we find that the resolution depends on the laser wavelength used and therefore the reduction of the wavelength of the laser increases the resolution of measurement. As shown in Fig. 3.1, the

scattered pattern is collected by a diode array detector. The received video signal can be serially clocked from the array at a rate of 1 KHz to analyze the fiber diameter.

Eq. (3.1) can also be used for clad fibers, but an error may be introduced for fibers having a large core.

The movement of the fiber causes a distortion in the received image as the image at θ_1 and θ_2 moves with the movement of the fiber. Increasing the window of fiber movement will increase the distortion of the received image which introduces increased error in fiber diameter measurements. Thus there is a trade-off between the size of the movement window and the amount of error that can be allowed in the fiber diameter measurement.

b) fiber diameter measurement using backward light scattering: Fig. 3.2 shows the experimental arrangement of a diameter measurement system using backward light scattering. The system is also valuable in finding the geometric configuration of the fiber. This technique analyses the back-scattered fringe pattern in an angular range of around ±20° about the incident direction. A CW He-Ne laser is incident on mirror M1 which reflects it to oscillating mirror M2, which helps in observing an extended length of fiber (typically ~7 cm), the length being determined by the amplitude of oscillation and the length of slit through which light is guided to impinge on the fiber.

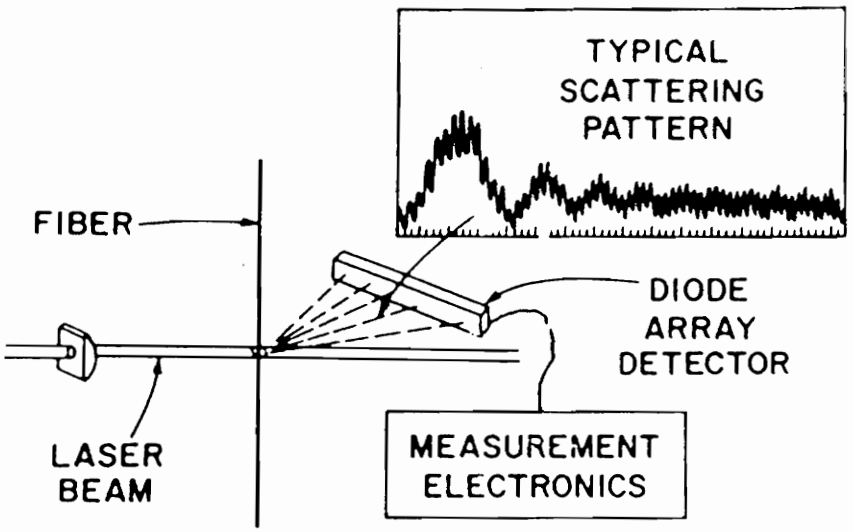

Fig. 3.1 Schematic of a diameter measuring arrangement using forward light scattering pattern [Jaeger et al., 1979].

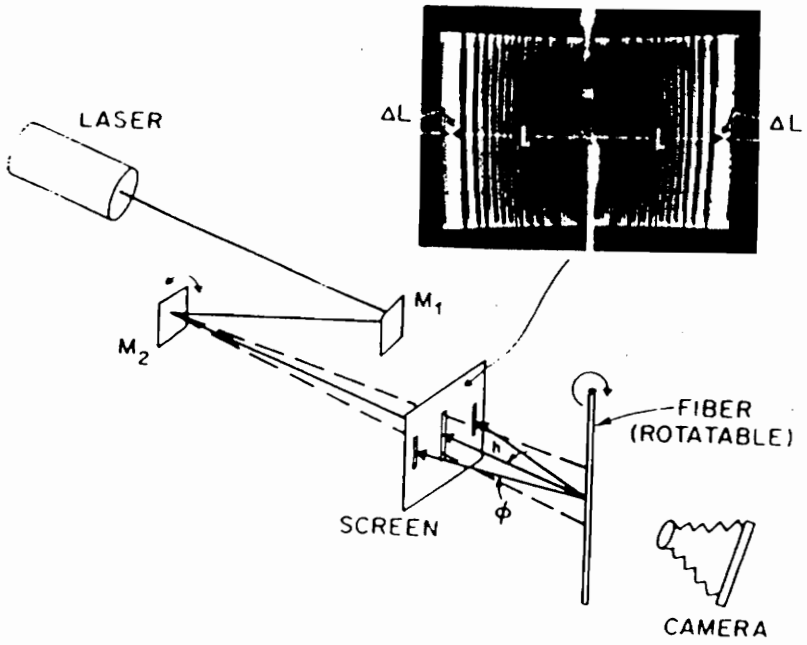

Fig. 3.2 Schematic arrangement of diameter measurement using backward light scattering [Jaeger et al., 1979].

c) fiber diameter measurement by polarized light scattering: Fig. 3.3 shows the experimental setup of a system of polarized light scattering, which can measure on-line fiber diameter as well as draw tension. Two light-emitting diodes (LEDs) emit unpolarized light which is polarized before it illuminates the fiber laterally. The scattered light is then passed through a focusing lens, quarter wave plate, and polarizers and then collected by photodetectors, as shown in the Fig. 3.3. The sum of the detected voltages after the two polarizers is proportional to the fiber diameter while the difference of the voltages is proportional to the draw tension [Chu et al., 1989]. Two LEDs are used instead of one to improve the lateral uniformity. Monitoring on-line fiber tension is very important to reduce the residual tensile stress and drawing dependent transmission losses. The direction of polarization of the incident ray on the fiber is 45° to the fiber axis, so that the light split in perpendicular and parallel directions to the fiber axis are equal. The thermal stress and the applied drawing tension make the fiber anisotropic so that the two orthogonal components suffer a phase retardation between them when traversing through the fiber [Chu et al., 1989].

The movement of the fiber in the field of view, introduces a considerable amount of inaccuracy in the fiber diameter measurement due to nonuniformity of the source, lens aberration, and the change in beam splitting ratio due to the change of angle of incidence [Chu et al., 1989].

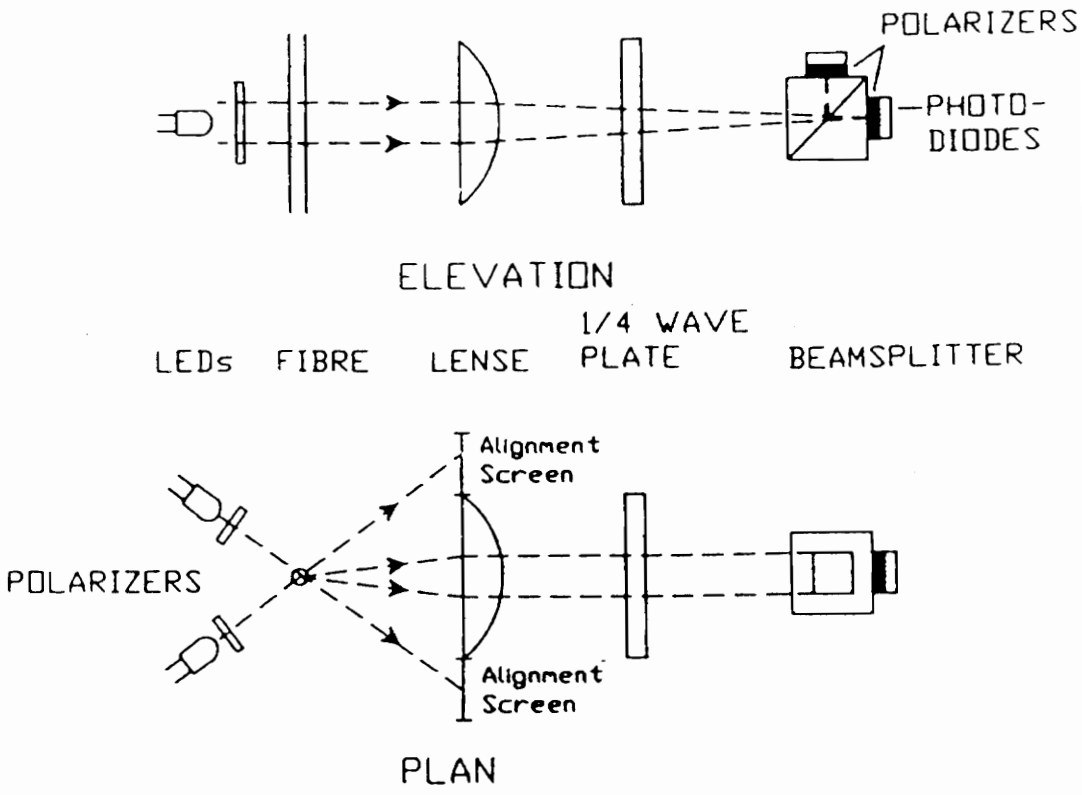

Fig. 3.3 Diameter measurement using polarized light scattering [Chu et al., 1989].

speed of the beam is known, the time during which the fiber intercepts the laser is proportional to its diameter. The intercepted time is the time required by the shadow of the fiber to eclipse a photo detector. This method is widely used in commercial applications to control fiber diameter. Obviously this method requires that the fiber axis maintain its position during measurements, to reduce the measuring error. The measuring error can also be reduced by increasing the scanning rate of the laser.

3.3 Diameter Measuring Accuracy as a Function of Fiber Movement

The first step in controlling diameter is to measure the on-line fiber diameter as accurately as possible. The accuracy of the fiber diameter measurement must be at least an order of magnitude higher than the precision with which the diameter needs to be controlled. For example, if the diameter of the fiber is to be controlled within ±1 μm of the nominal value, the diameter measuring accuracy must be at least one tenth of a micrometer.

As discussed in Section 3.2, the movement of the fiber is the major source of error in on-line fiber diameter measurements. The bends in the preform, asymmetric neck-down shape, mechanical and acoustic vibrations can cause the fiber to move laterally in its measuring window. The movements due to bends in the preform or asymmetric neck-down shape are slow in time while the movements due to vibrations are very fast. It is difficult to control very fast and short scale movements of vibrations, while it is possible to control or avoid slow and large scale movements. This control can be achieved by applying a feedback to the preform X-Y position from the diameter measuring system which can give an output of lateral position of the fiber with respect to its center of the measuring window.

3.4 A Detailed Experiment with a Diameter Measuring System

We conducted experiments on a commercial on-line fiber diameter measuring system, Anritsu M551A, to dtermine the variations in diameter measurement moving the fiber, laterally, at different positions within its measuring window. We found a wide variation in measured diameter of the same fiber when the fiber is moved laterally within the measuring window. Also an offset in the measurement has been observed when the diameter measuring system is calibrated with metalic standards. The following sections give a detailed discussion of the system and the experiments.

3.4.1 Anritsu M551A

Anritsu M551A SLB DIA-MEASURING SYSTEM is a non contact diameter measuring system which uses the scanning beam technique described in Section 3.2. It consists of two units, the OPTICAL UNIT and the PROCESSING UNIT. The OPTICAL UNIT has an oscillating laser beam which scans the object of interest. The PROCESSING UNIT determines the diameter of the object by measuring the time taken by the shadow of the fiber to eclipse a photo detector. The instrument has the following features [Anritsu , 1984]:

i) The non-contacting and reversible scanning method, using a vibrating mirror at the top of the tuning fork, allows stable measurement of moving objects.

ii) The scanning rate of the laser beam is 1000 scans/sec and the analog signal of the measured diameter is provided with maximum response of 2 milli seconds.

iii) The accuracy is maintained within limit even if the object moves within the measuring area.

iv) Diameters are digitally displayed and deviation from a nominal diameter is available in the form of analog voltage.

v) The instrument can be calibrated by either Single Point Calibration or Double Point Calibration using a single standard wire or two standard wires respectively. For single point calibration the accuracy is guaranteed only near the standard wire diameter and for double point calibration the accuracy is maintained all through the range of the standard wires.

vi) The influences of ambient light and intensity variations of the laser are very small. Sufficient stabilization is provided to prevent the drift resulting from temperature changes.

vii) The position of the object within the measuring area can be two-dimensionally monitored during the measurement of diameter.

viii) The instrument can be controlled remotely by means of the General Purpose Interface Bus (GP-IB).

Anritsu M551A specifications:

Measuring range:	50 μm to 1 mm
Measuring area:	2 mm X 3 mm

Repeatability:	50 t0 300 μm	0.3 to 1 mm
at definite position	±0.1 μm	±0.1 μm
within measuring area	±0.2 μm	±0.3 μm
Linearity:	±0.5 μm	±0.5 μm
Measuring rate:	1000 times/sec	
Averaging rate:	2, 4, 8, 16, 32, 64, 128, 256	
Nominal diameter :	4 digits (step of 0.1 μm)	
Higher and lower limiter:	3 digits	
Outside diameter:	6 digits (step of 0.05 μm)	
Refreshing period:	0.13 sec	
I/O interface:	GP-IB (IEEE-488)	
Analog output:	Max. voltage: ±10 V	
	Max. current: ±5 mA	
	Output impedance: < 1 Ω (DC)	
	Deviational: 125 mV/μm	
	Absolute value: 5 mV/1.28 μm	
Object position:	Display: 5 X 5 LED's matrix	
	Analog output accuracy:	
	Transverse (Y) ±2%	
	Axial (X) ±25%	
	Along transverse direction:	
	±1 mm/±10 V	
	Along axial direction:	
	±1 mm/±5V	
Status monitor LED:	1) Laser intensity of transmitter	

	2) Laser intensity of receiver
	3) Higher limiter
	4) Lower limiter
	5) Communication interface bus: REMOTE, SRQ, TALK, LISTEN
	6) Calibration
Alarm signal:	1)Setup error (laserintensity/object position)
	2) Over the higher limit
	3) Under the lower limit
Operating temperature:	0 to 40 °C
Warm-up time:	30 minutes maximum
Power requirement:	100, 115, 220, 240 V AC ±10%, 50/60 HZ, 150 VA
Dimension and weight:	Processing unit: 426 x 351 x 133 mm, 8 kg
	Optical unit: 340 x 190 x 90 mm, 6 kg

Fig. 3.4 shows the processing unit and Fig. 3.5 shows the optical unit of Anritsu M551A. To calibrate the system the standard in mounted on the base plate, in which the standard can be moved in both X and Y directions, as shown in Fig. 3.5.

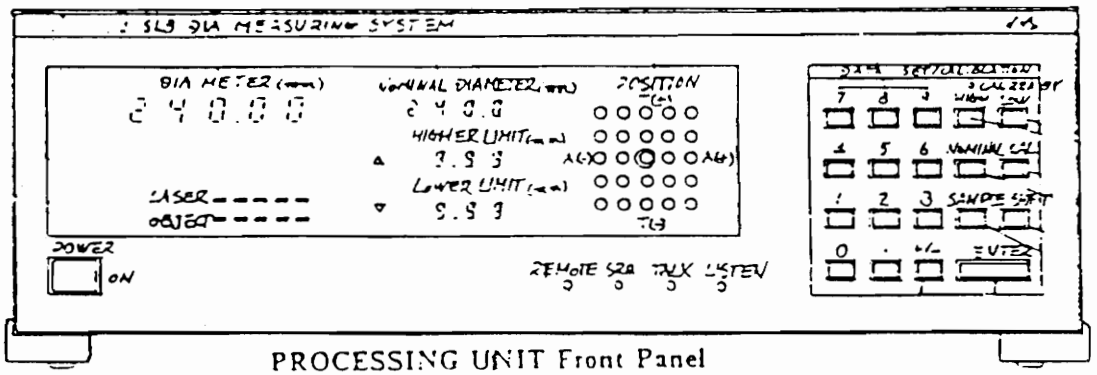

PROCESSING UNIT Front Panel

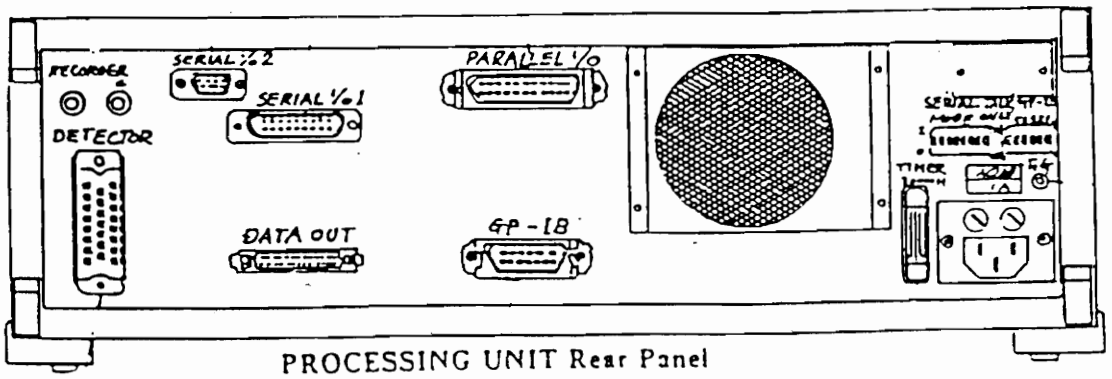

PROCESSING UNIT Rear Panel

Fig. 3.4 Anritsu M551A Processing Unit [Anritsu, 1984].

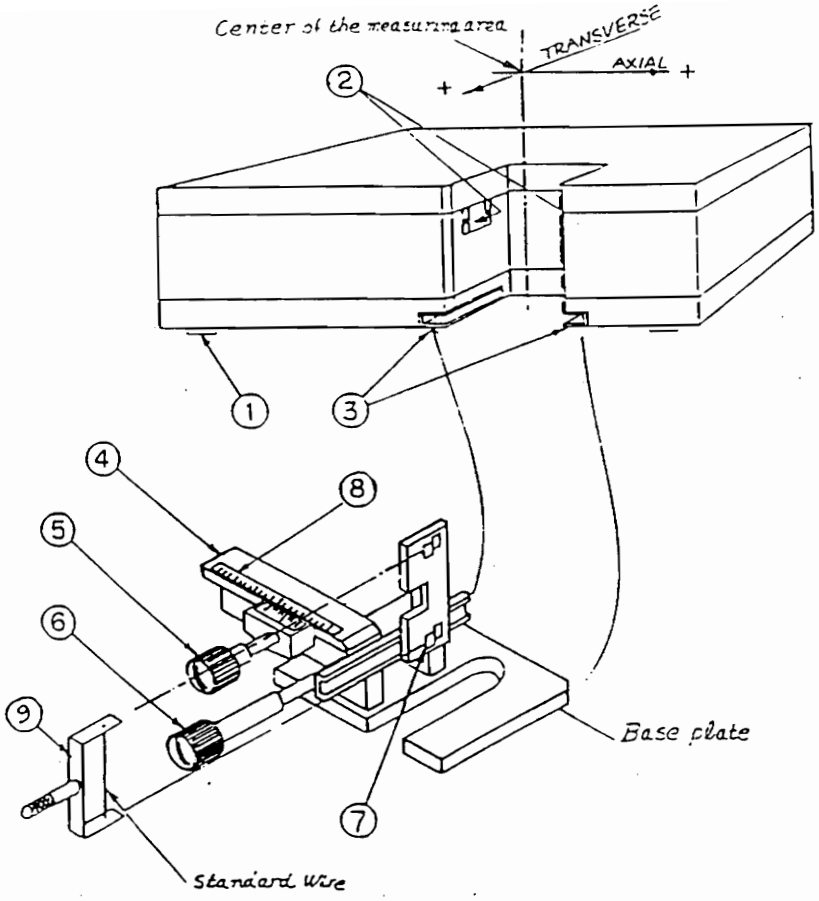

1. Feet which support the OPTICAL UNIT
2. Filters to protect the optical components from the contaminations
3. Mount guide for the mechanical stage
4. Mechanical stage to adjust position of the standard wire to the center of the measuring area
5. Knob to move the standard wire along the laser beam direction
6. Knob to move the standard wire along the direction of scanning
7. Leaf springs to support the standard holder
8. Positioning scale
9. Standard holder

Fig. 3.5 Anritsu M551A Optical Unit [Anritsu, 1984].

3.4.2 Experiments with M551A

The Anritsu M551A uses the scanning beam technique to measure the fiber diameter, as described in Section 3.2. The beam scans the fiber at a rate of 1000 Hz. The fiber must be within the measuring window, which is 2 mm X 3 mm, to be scanned and measured by the system. It has been observed that the measured diameter is not independent of fiber location within the measuring window. The diameter measurement has considerable amount of variation with the change of fiber position within the measuring window. We tested Anritsu M551A units to find the variations of the measured diameter, by placing a standard fiber on the base plate and then moving the fiber either in X, or in Y, or in both axis, within the scanning area of the optical unit. Fig. 3.6 to Fig. 3.11 shows the results of the experiments. The positional signals, a dc analog voltage output proportional to the position of the fiber in X and Y axis, are also shown. There are two separate analog outputs one for X axis position and the other for Y axis position. The zero analog output of an axis indicates that the fiber is at the center of that axis.

It is obvious from Fig. 3.6 to Fig. 3.11 that for an accurate measurement of diameter, it is not sufficient that the fiber be within the measuring window. Rather it also requires that the fiber be always at the center of the measuring window.

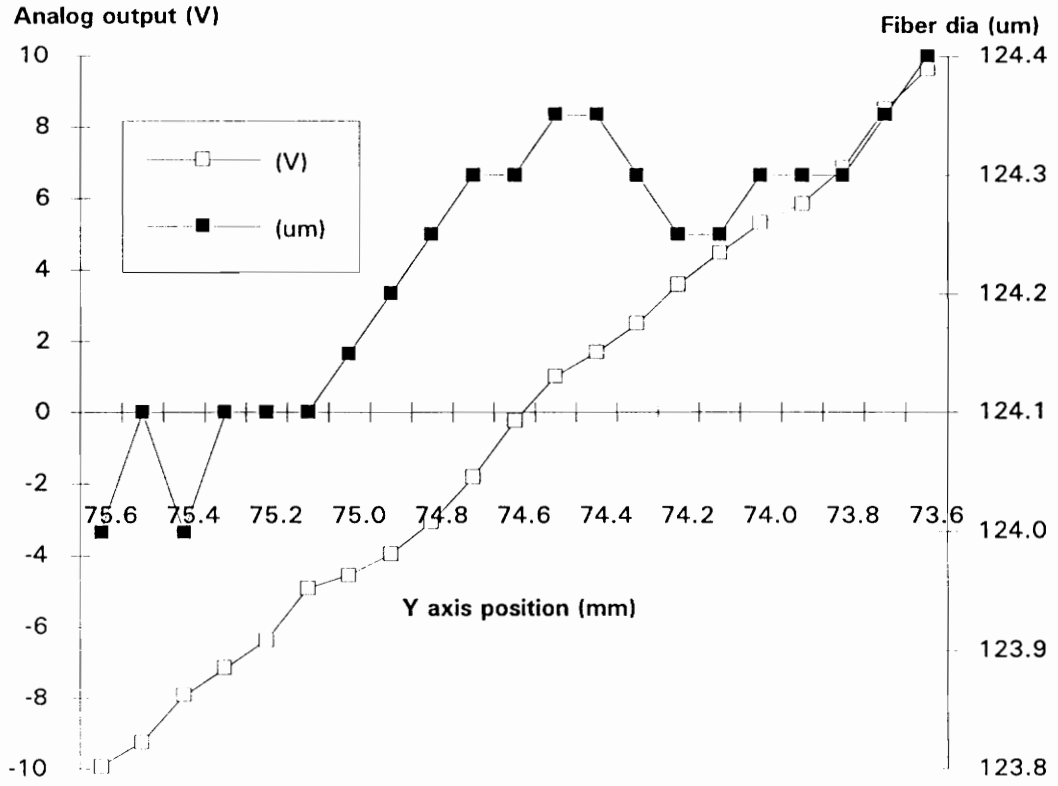

Fig. 3.6 Variation of measured diameter with the Y axis positional change of fiber, X axis remaining fixed. Analog outputs corresponding to Y axis positions are also shown.

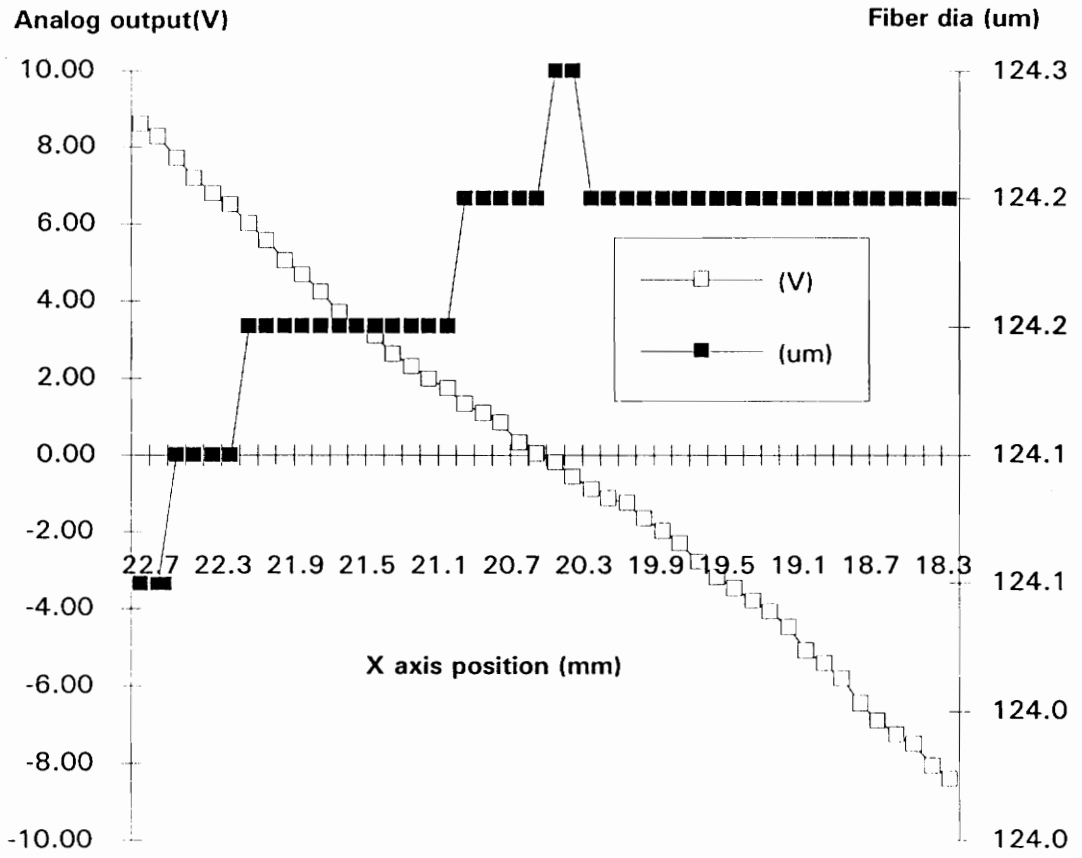

Fig. 3.7 Variation of measured diameter with the X axis positional change of fiber, Y axis remaining fixed. Analog outputs corresponding to X axis positions are also shown.

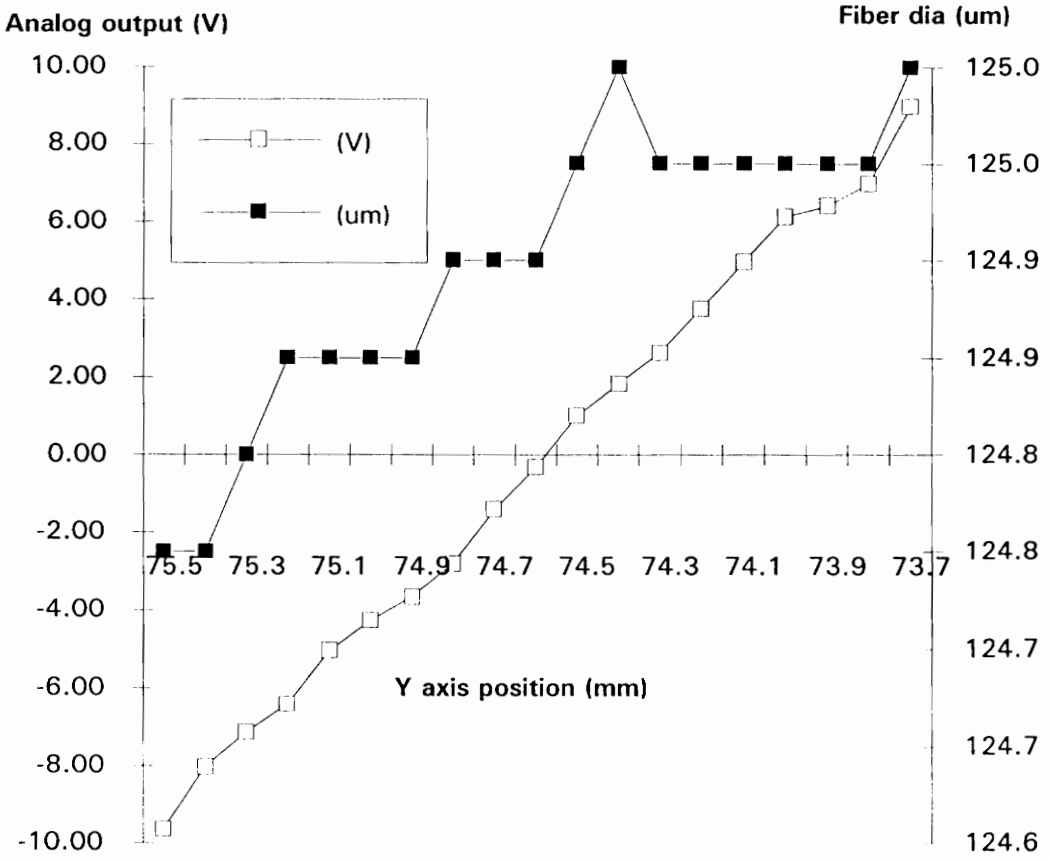

Fig. 3.8 Variation of measured diameter with the Y axis positional change of fiber, X axis remaining fixed. Analog outputs corresponding to Y axis positions are also shown.

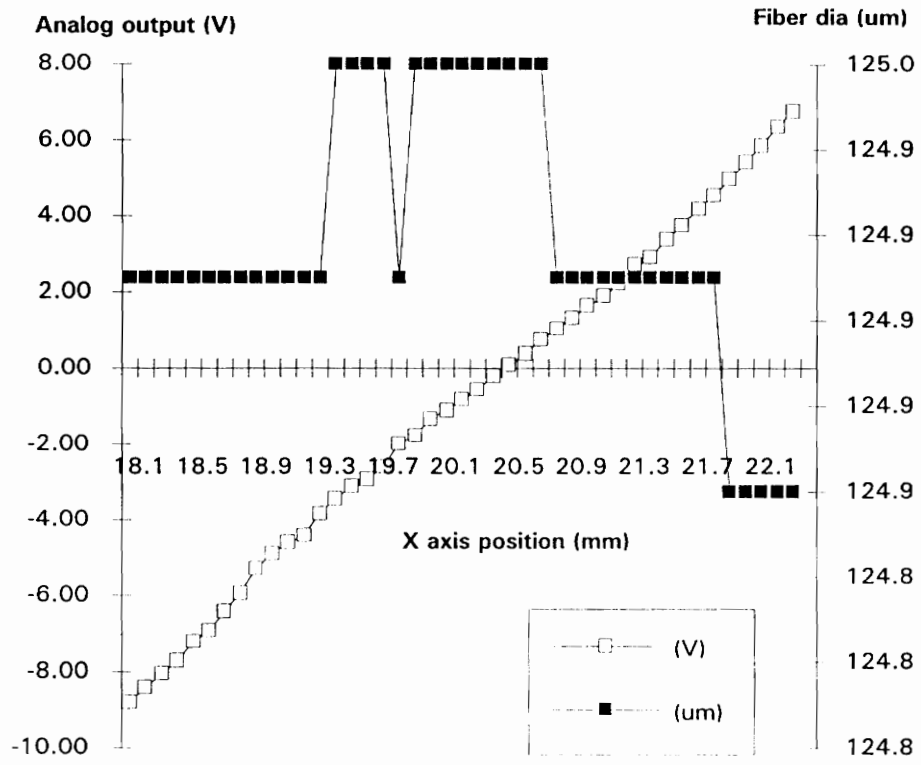

Fig. 3.9 Variation of measured diameter with the X axis positional change of fiber, Y axis remaining fixed. Analog outputs corresponding to X axis positions are also shown.

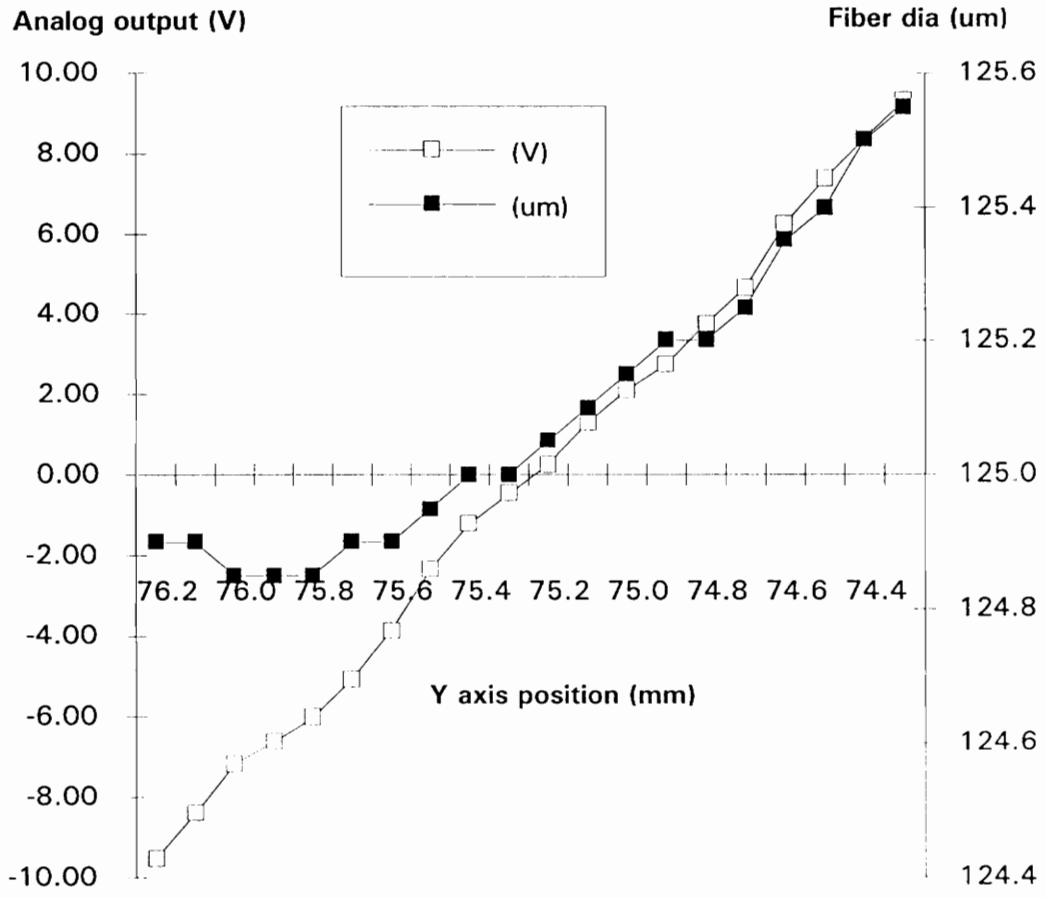

Fig. 3.10 Variation of measured diameter with the Y axis positional change of fiber, x axis remaining fixed at the center. Analog outputs corresponding to Y axis positions are also shown.

X axis position vs fiber dia (Anritsu unit 114141, single point calibration)

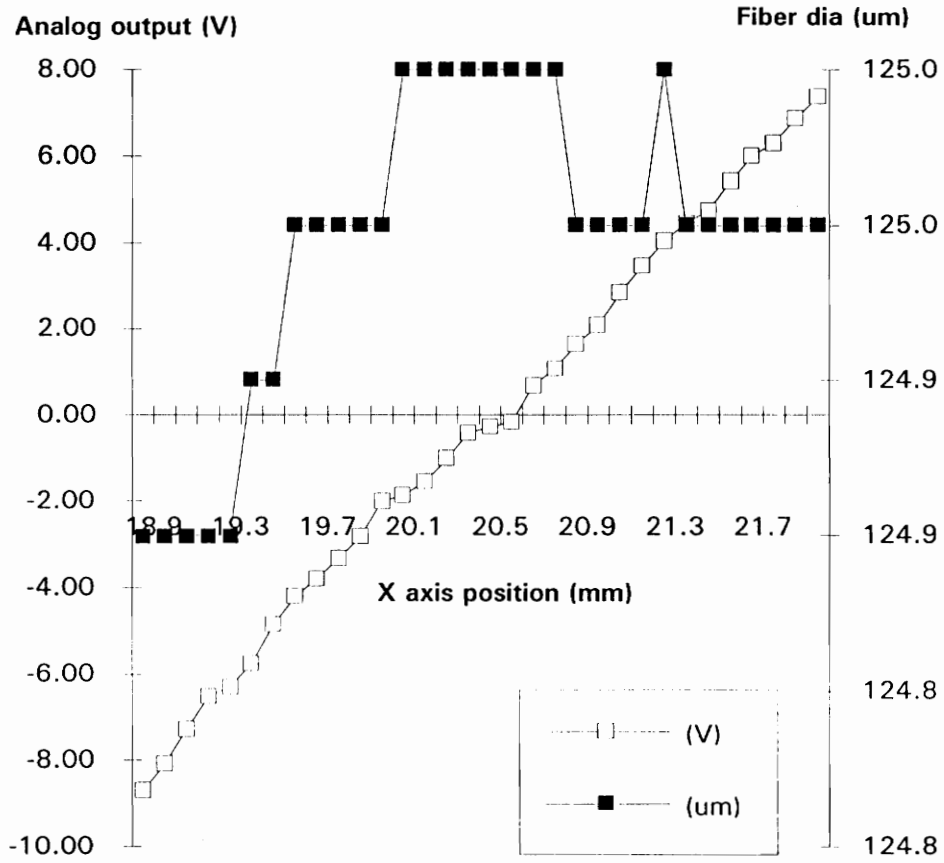

Fig. 3.11 Variation of measured diameter with the X axis positional change of fiber, Y axis remaining fixed. Analog outputs corresponding to X axis positions are also shown.

3.4.3 Glass standard versus metallic standard

The Anritsu M551A is usually calibrated with metallic standard wires (of known diameters), which introduces an offset in the measurement of glass fibers which are unlike metallic wires. The system shows a diameter for glass fiber which is smaller than its actual value, when calibrated with metallic standard wires. This variation has also been observed by Baines et al. [Baines et al., 1990]. Fiber with metallic coating showed no offset and was in good agreement with its actual diameter. So it is obvious that the offset in the diameter measurement of glass fiber can be avoided if glass standards are used for calibration. We have developed a procedure of making glass standards, out of optical fiber itself, which is discussed below.

3.4.4 A procedure of making glass standards

The following specifications describe a procedure to make glass standards for calibrating the Anritsu M551A diameter measuring system. It uses PHOTON KINETICS 2400 to measure the end-face diameter of the fiber. It is more precise in diameter measurement compared to on-line measuring systems like Anritsu M551A.

a) Selecting fiber pieces for making standards:

i) Obtain samples of fiber, from spools which have little variation in their diameter, each approximately a meter in length (a minimum length of about two feet is required to measure the diameter using PHOTON KINETICS MODEL 2400). Measure the diameters of both the ends of the samples using the standard measuring procedure. Select several of samples which have both the ends very near to 125.00 μm (e.g. 124.90

μm to 125.10 μm). We want to make a 125 μm standard as the on-line fiber has a nominal diameter of 125 μm.

ii) Measure an end of a particular sample at least four times, each time placing the fiber at a different orientation to the scanner (e.g. by rotating the fiber a little bit inside the holder).

iii) Cut about two inches from the measured end of the fiber and preserve the cut piece on a white paper fixed with a bit of masking tape, as shown in Fig. 3.12. Measure the cut end of the fiber piece again, at least four times, while keeping the other end intact. Record all the measured diameters and their ovalities on the white paper to the corresponding end of the cut piece, as it might be selected as a standard later on.

iv) Repeat step a(iii) several times and if the diameter of the fiber seems to not be varying considerably (e.g. not more than ±0.1μm) with length then a piece may be selected as a standard provided:

1) all the end face measurements of the piece are very close to one another (e.g. the variation is within ±0.1μm) and

2) the ovality of each measurement is low (e.g. not more than 0.12) i.e. the maximum and the minimum diameter measured of each measurement are very close to each other (e.g. within 0.15μm).

v) If the diameter of the fiber seems to vary considerably (e.g. more than 0.1μm) with length then discard that fiber and start from step a(ii) taking another sample of fiber.

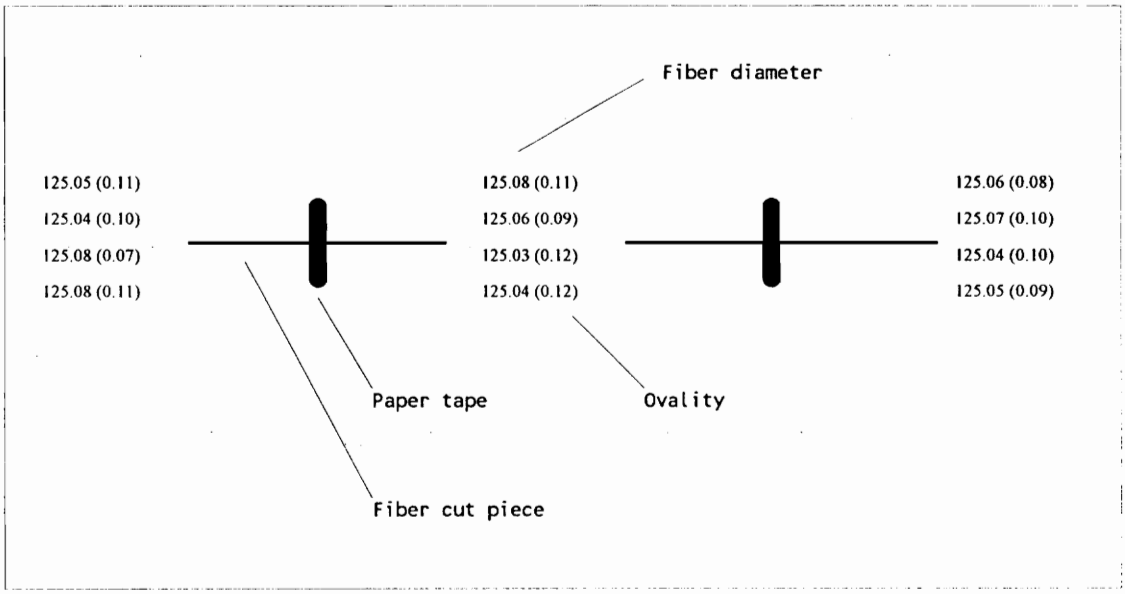

Fig. 3.12 Probable glass standards.

vi) Make many (about ten to twenty) pieces that may be used as standards.

b) Comparing the selected pieces with each other using the Anritsu unit and fixing them to the standard holder:

i) Take a sample of fiber and fix it temporarily on a standard holder, as shown in Fig. 3.13. A piece can be fixed temporarily by blocking the lower side of the bottom hole of the standard holder with a bit of masking tape and then sliding the piece through both the holes such that it is blocked at the lower side of the bottom hole. As the fiber is light in weight it sticks to the masking tape at the bottom end and does not fall down even when the standard holder is flipped over.

ii) After fixing the fiber temporarily, clean it very carefully with propanol solution, as it may gather some dust particles even while passing through the hole, and let it dry.

iii) Calibrate the Anritsu unit with the fiber piece (taking the average of all the end face measurements as its diameter) using single point calibration. Anritsu can be calibrated with an accuracy of only one tenth of a micron.

iv) Measure all other pieces, fixing temporarily on the standard holder, with the same calibration and compare the displayed diameter with the diameter measured from the measurements. Take several (e.g. four) measurements for each piece rotating the piece little bit (e.g. 90°) after each measurement.

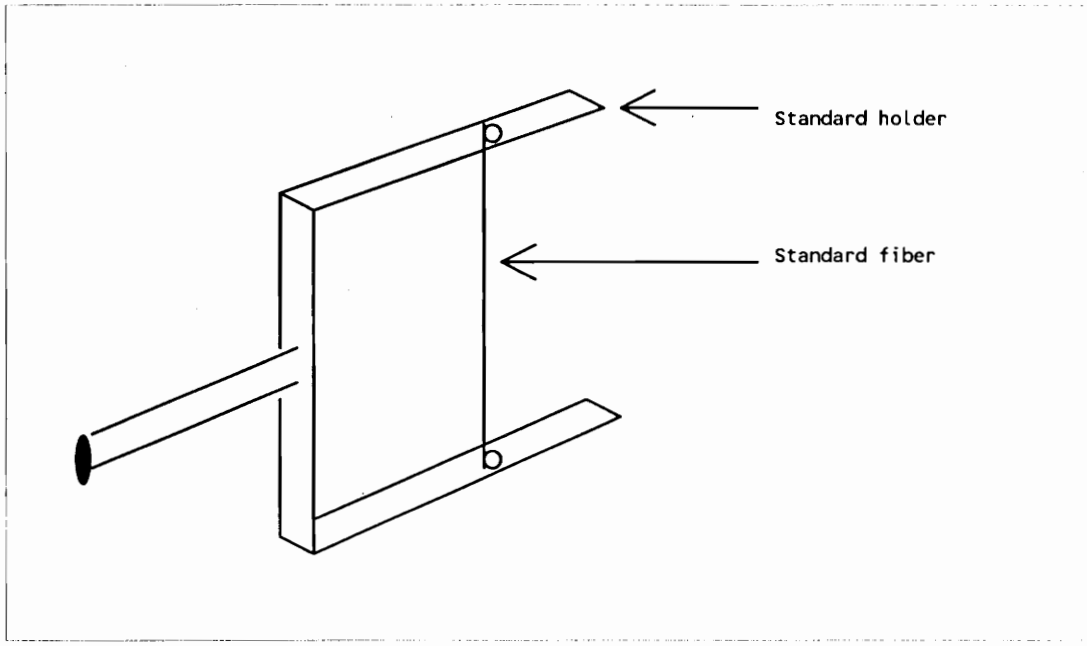

Fig. 3.13 Standard fiber holder.

v) There may be variations of the displayed diameter with the slight changes of the fiber position while the fiber position in the LED display still reads the center position. So, calibrate and take measurements only when the analog outputs of both pin 8 (which indicates the object position along transverse, X axis, direction with a voltage range of ± 10 volts) and pin H (which indicates the object position along axial, Y axis, direction with a voltage range of ±5 volts) from the rear panel DATA OUT of the PROCESSING UNIT are zero volts (or very near to zero volts). Pin 12 and 13 of DATA OUT are the ground for the analog signal.

vi) Step b(i) through b(iv) can be performed several times each time using a different standard fiber for calibrating the Anritsu unit. If the displayed diameter varies considerably (e.g. more than 0.15μm) with its rotation or if the diameter displayed is inconsistent with its measured diameter and the displayed diameters of the other selected pieces then the corresponding piece should be discarded.

vii) If a piece is consistent in all the measurements, it can be selected as a standard. To fix the piece permanently first fix it temporarily as described earlier and then put a small spot of epoxy in the bottom hole of the standard holder and let it cure. Cut the end of the piece which stands out of standard holder. It is better to fix only one side with epoxy and let other side be free, because then even if the standard holder is compressed or expanded the standard fiber will not experience any stress or tension.

The biggest problem with glass standards is its fragility. It may develop microcracks or invisible scratches on the surface making it an unreliable standard. To avoid this problem the standard must be handled very carefully and be preserved in a dust free shock absorbent cushioned case.

3.4.5 Feedback to preform X-Y position to place the fiber at the center of the diameter measuring window

As it has been shown earlier, the diameter measured by the Dia Measuring System depends on the position of the fiber within the measuring window. For accurate measurement of the on line fiber it is very important that the fiber be always kept at the center of the measuring window. The X and Y axis positional signals of the fiber within the window are available from the diameter measuring system. These signals can be used as a feedback to the preform X-Y unit to keep the fiber always at the center of the measuring window.

Fig. 3.14 shows a feedback system, using a PLC, which tries to keep the fiber to the center of the measuring window. The feedback provided to the preform X-Y unit is not continuous and is controlled by a PLC. There are independent feedbacks for the X and the Y axis positions of the fiber within the measuring window. The feedback is provided only if the fiber is away from the center position of either axis by a predetermined distance. Once the feedback is started for a particular axis it is continued until the fiber is at the center position of that axis and then the feedback is stopped. A continuous feedback increases the vibration of the preform and increases diameter variation rather than reducing it. We implemented the feedback system as shown in Fig. 3.14, as a prototype, in a draw tower of Alcatel NA Cable System, Roanoke. The prototype system produced better results in controlling fiber diameter and a decision was made to implement the system to all the towers of Alcatel's Roanoke plant. The type of PLC used for the system and also the software used to program the PLC has been given in the Appendix of this thesis.

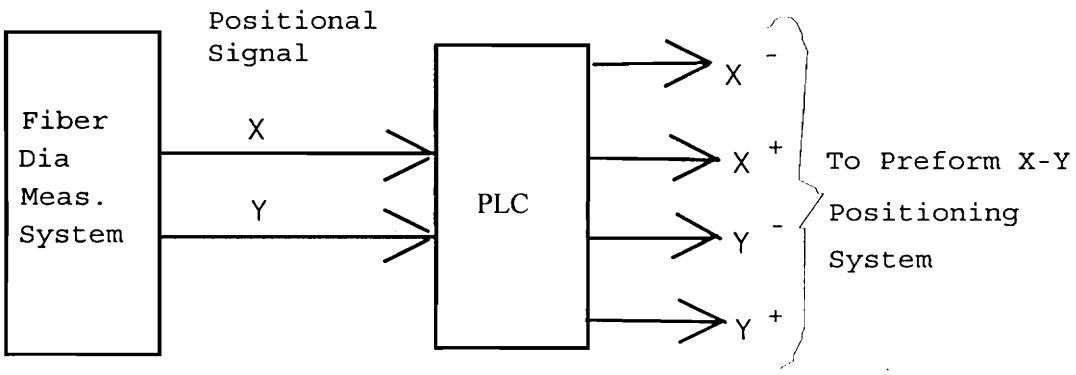

Fig. 3.14 Preform X-Y feedback system using PLC.

CHAPTER 4

COATING

4.1 Purpose of Fiber Coating

Silica fibers are inherently very strong, with tensile strengths of approximately 7 GN/m^2 (10^6 psi) in air and 14 GN/m^2 in liquid nitrogen [Paek, 1986], and is actually one of the strongest materials known. But the problem is that the surface of the fiber is very sensitive to external influences. By coming in contact with a foreign particle or matter, it can easily develop surface cracks or damages, which reduce its strength drastically. The main purpose of applying a coating on fiber is to protect its surface from surface damage and moisture so that it can preserve its intrinsic strength. The coating allows the fiber to retain its original strength and makes it more flexible to handle.

Coatings may also be designed to reduce the microbending losses. Making random small radius bends in the fiber axis and measuring losses induced by the bends, it has been found that the fibers coated with polymer having low modulus of elasticity yield considerably less microbending losses compared to than uncoated fibers [Gardner, 1975].

The coating must be applied uniformly, and continuously. Lumps, voids, foreign particles in the coating can decrease the fiber strength and introduce losses. The coating must be applied to the fiber on-line, immediately after it is being drawn from the furnace, to decrease the exposure time of the fiber to

open environment. On-line coating appliccation also requires that the coating must be cured very rapidly before it reaches to the winding capstan.

4.2 Coating Fluid

The characteristics and purity of the coating fluid greatly influence the strength and transmission properties of optical fibers. Coating fluids can be of two types: (a) organic material, such as UV curable polymer or thermally curable resin and (b) inorganic material, such as metallic coating. Because of their low modulus of elasticity and rapid solidification at low energy, UV curable polymers are most extensively used for commercial production of optical fibers.

To obtain high performance fiber, the coating fluid must meet specific criteria. Among them are [Dimarcello et al., 1985] [Cocito et al., 1981],

i) low modulus of elasticity,

ii) good abrasion resistance,

iii) rapid solidification at low energy,

iv) good bonding to glass,

v) good moisture resistance,

vi) proper index of refraction,

vii) ease of coating removal for cutting and splicing operations,

viii) high chemical stability,

ix) proper viscosity, and

x) free from bubbles or dust particles.

The coating fluid should also have very high critical shear rate for high-speed smooth coating. At the critical shear rate the shear fracture begins to occur and the maximum smooth coating speed corresponds to the coating speed at which the shear fracture begins to occur [Wagatsuma et al., 1982]. Above the maximum smooth coating speed, the coating thickness fluctuation begins to increase abruptly due to the fracture of the coating fluid caused by shear.

4.3 Coating Applicator

The coating thickness and uniformity are mainly governed by the geometry of the coating applicator. Fig. 4.1 shows the geometry of typical coating applicator. The motion of the fiber drags the coating fluid through the nozzle. For a plain cylindrical nozzle and steady incompressible flow along the axis of the cylinder, the coating thickness, t, is determined as [France et al., 1979],

$$t = \left\{ a^2 + \frac{1}{\ln b/a} \left[\frac{b^2 - a^2}{2} - a^2 \ln b\sqrt{a} \right] \right\}^{1/2} - a \quad , \tag{4.1}$$

where $2a$ is the fiber diameter and $2b$ is the nozzle diameter. Eq. (4.1) indicates that the coating thickness is independent of draw speed and fluid viscosity and it decreases slowly with increasing fiber diameter under typical operating conditions.

In addition to a uniform coating diameter, the coating must also be concentric around the fiber to achieve its maximum performance. Fibers coated from a straight-sided cylindrical nozzle are often nonconcentric, as there are no centralizing forces acting on the fiber except the weak end effect forces which apply for Newtonian fluids.

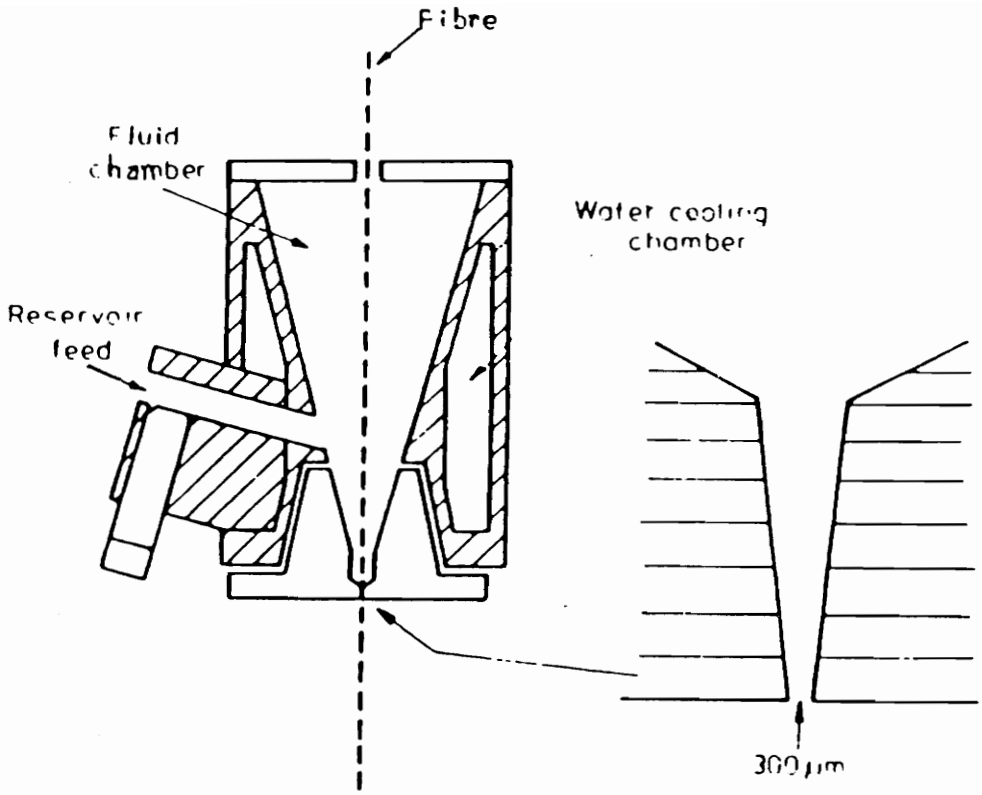

Fig. 4.1 Geometry of a typical coating applicator [France et al., 1979].

A conical nozzle is essential for obtaining a concentric coating. The fluid flow in a conical nozzle induces a force which automatically centers the fiber and makes the coating concentric. The restoring force on the fiber, F, that tries to bring it to the center is given as [France et al., 1979],

$$F = \frac{a}{\alpha} \int_0^{2\pi} \int_{b_1}^{b_2} (P \cos\beta) db d\beta \quad , \tag{4.2}$$

where,

$$P = \frac{6\mu V_f}{\alpha} \left\{ \frac{(H - H_1)(H - H_2)}{(H_1 - H_2)H^2} \right\} \quad , \tag{4.3}$$

and,

$$H = \left(b^2 - e^2 \sin^2/\beta\right)^{1/2} + e\cos\beta - a \quad , \tag{4.4}$$

as shown in Fig. 4.2. H_1, H_2 are H evaluated at the die ends.

Solving Eq. (4.2) and differentiating it with respect to α and then equating it to zero, the angle of taper of the conical nozzle for the maximum restoring force can be determined. Fig. 4.3 shows the restoring force as a function of angle of taper for the parameters shown, the maximum restoring force being at an angle of taper of 2°.

The coating thickness, t, of a fiber drawn from a conical applicator can be found using [Paek, 1986] [Chida et al., 1982],

$$t = \sqrt{a^2 + \frac{Q}{\pi V}} - a \quad , \tag{4.5}$$

where $2a$ is the fiber diameter, V is the coating speed and,

$$Q = 2\pi \int_a^R urdr \quad , \tag{4.6}$$

where R is a function of z and describes the conical shape varying in the radial direction r along the axis. u is the velocity component of the fluid in the axial direction (z axis) and is given by [Paek and Schroeder, 1979],

$$u = \frac{1}{4\eta}\left(r^2 - R^2\right)\frac{dp}{dz} + \frac{\ln(r/R)}{\ln(a/R)}\left\{V - \frac{1}{4\eta}\left(a^2 - R^2\right)\frac{dp}{dz}\right\}, \tag{4.7}$$

where η is the viscosity of coating fluid and $\frac{dp}{dz}$ is the pressure gradient.

4.4 Cure of Coating

The coating must be cured completely before the fiber reaches the winding capstan, otherwise fibers will stick to each other and can not be separated from the winding. There are usually two types of curing methods: (a) thermal curing and (b) UV radiation induced curing, the latter being mostly used in industries due to specific advantages. In thermal curing, a tubular oven supplies energy to thermoplastic resin type coating fluids to make it solidify before the fiber reaches the capstan. The UV radiation induced curing is actually a photopolymerization technique, which uses UV radiation to initiate a chain reaction and form cross linkage of preexisting monomer molecules. This system is very efficient and can be designed with a compact reflector which delivers high intensity radiation to the coating fluid.

The UV induced photopolymerization process can be devided in three steps: initiation, propagation and termination. In the first step the iniator (S) absorbs the photon ($h\nu$) and if the absorption energy is sufficient enough it breaks the chemical bonds of molecules and makes free radicals. The absorption and breaking process can be expressed by [Walker et al., 1970],

$$S + h\nu \rightarrow S^* \ ,$$

$$S^* \rightarrow 2R\bullet \ , \tag{4.8}$$

where $h\nu$ indicates the energy of the photon and $R\bullet$ indicates the free radical.

These radicals and monomer M reacts rapidly and progressively grow a chain to crosslink into the polymer network,

$$M + R\bullet \rightarrow RM\bullet$$

$$RM\bullet + M \rightarrow RMM\bullet. \tag{4.9}$$

This propagation continues until it is terminated by a reaction with a hydrogen atom.

The total UV power required to cure a coating of thickness $t = h - a$, on a fiber that is drawn at a speed V_f, can be formulated as [Paek and Schroeder, 1981(April)],

$$P = \pi \Delta E [C](h^2 - a^2) V_f \ , \tag{4.10}$$

where ΔE is the activation energy of a photoinitiator and $[C]$ is the concentration of photoinitiator in the fluid. $2h$ and $2a$ are the coated and bare fiber diameters, respectively. Usually the photoinitiator level in the fluid is about 3-5% and the choice of the optimum concentration depends on resin formulation and light sources. For a typical example, putting ΔE =70Kcal/mole, $[C]$=2X10^{-4}mole/cm^3 and h=225μm, we get,

$$P = 1.6 V_f \ , \tag{4.11}$$

where P is in watts and V_f is in m/sec. Note that Eq. (4.11) gives the power absorbed in the coating fluid, not the power produced by the UV lamp.

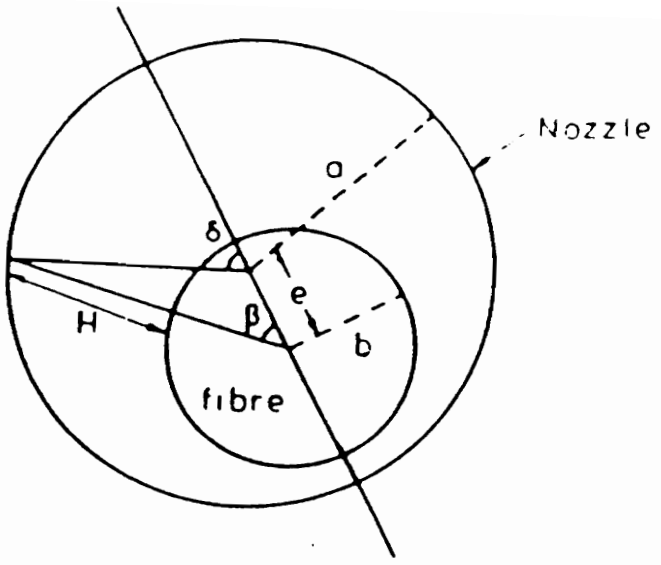

$$H = (a^2 - e^2 \sin^2\beta)^{1/2} + e\cos\beta - b$$

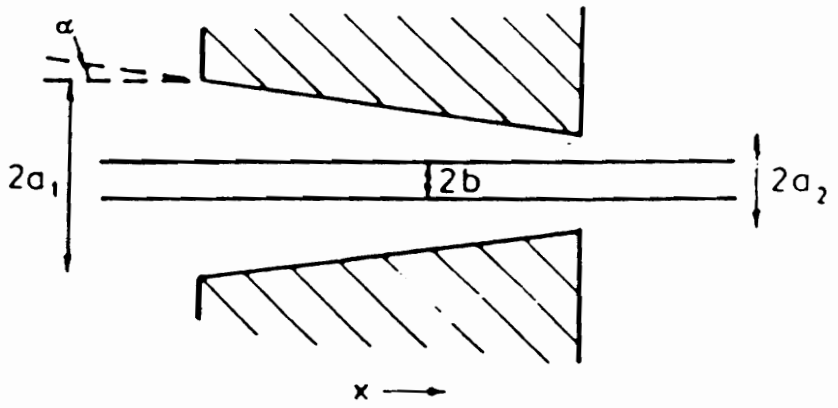

Fig. 4.2 Tapered nozzle and the fiber [France et al., 1979].

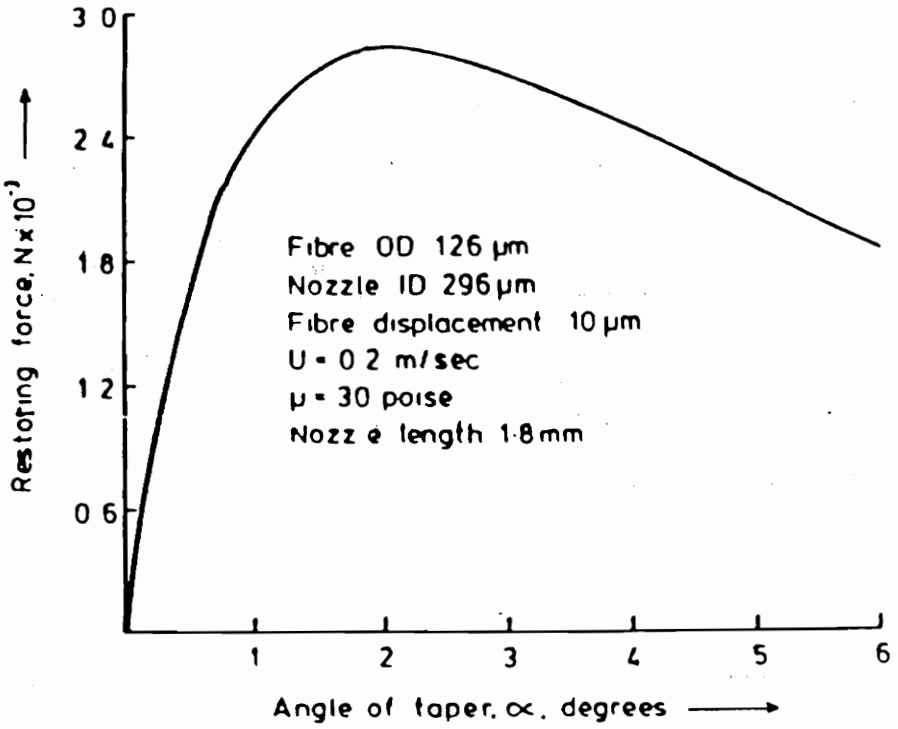

Fig. 4.3 Fiber restoring force versus angle of taper [France et al., 1979].

4.5 High-speed Coating

In modern processes the draw speed of optical fiber is very high, up to 20m/sec. The draw speed is kept high mainly due to two reasons: (1) better performance fibers are achieved if drawn at higher speed and (2) high-speed drawing reduces the overhead production cost. But high-speed drawing also implies high-speed coating. High-speed coating demands special considerations in designing the draw system. The main features of a high-speed coating process are:

a) Cooling of optical fiber: In high-speed coating the time gap between when the fiber leaves the furnace and when the fiber reaches the coating cup is very small. So, it must be considered that a very hot fiber enters the coating cup. But, if the fiber temperature exceeds about 300°C it may deteriorate or even char the coating fluid [Paek and Schroeder, 1979]. To avoid this problem either sufficient distance between the furnace and coating cup must be provided to self-cool the fiber while it is being drawn or a forced cooling system must be provided between the furnace and the coating cup to keep the fiber temperature at a safe level when it enters the coating fluid.

Fig. 4.4 shows the schematic of a high-speed coating process using a self-cooling technique. It also shows a coordinate system, used in calculating the fiber temperature at any distance along its axis. z is the distance along the axis of the fiber; z=0 at the end of the neck-down region where the fiber diameter is at its steady value and where the fiber temperature is at the lower softening point T_S (~1600°C). The fiber temperature, T, at any distance z, can be calculated by using the relation [Oh, 1979],

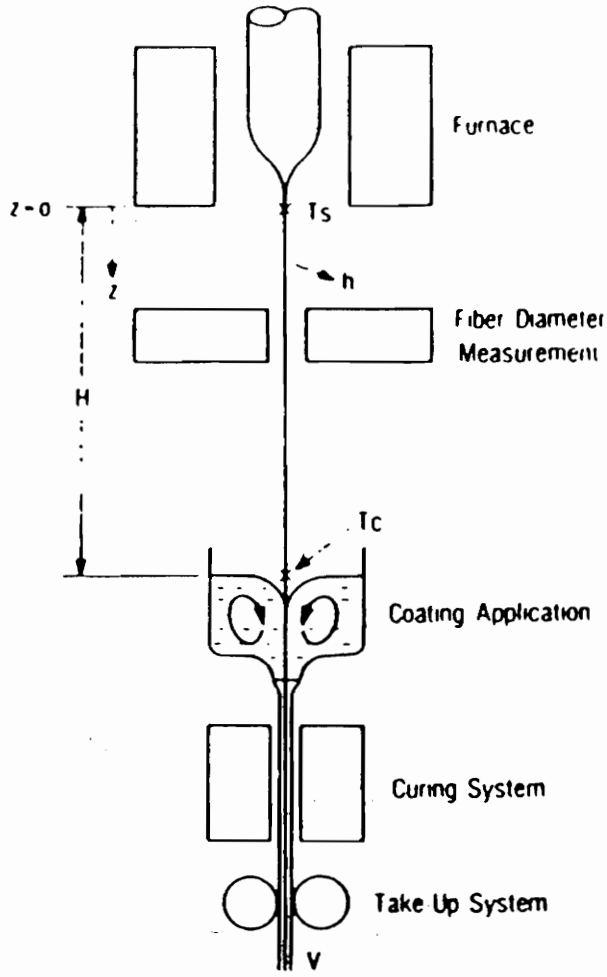

Fig. 4.4 Schematic of a high-speed coating process using self-coding technique [Paek, 1986].

$$T = T_0 + (T_s + T_0)\exp\left[-\frac{2hz}{a\rho C_p V_f}\right], \tag{4.12}$$

where T_0 is the ambient temperature, h is the heat transfer coefficient, $2a$ is the fiber diameter, ρ is the density, C_p is the specific heat and V_f is the draw speed.

Now, if T_c is the maximum fiber temperature that can be allowed to enter the coating fluid, the minimum distance, $z=H$, required for the fiber to self-cool can be easily obtained by using Eq. (4.12),

$$H = \frac{a\rho C_p \theta}{2h} V_f, \tag{4.13}$$

where

$$\theta = \ln\left(\frac{T_s - T_0}{T_c - T_0}\right). \tag{4.14}$$

Eq. (4.13) indicates that the distance of the coating cup is directly proportional to the coating speed. Therefore, a tall draw tower is needed to incorporate a high-speed coating system.

If a forced cooling system is implemented by blowing cool air across the fiber along its axis, it can be assumed as a superposition of two different fluid flows, namely axial and cross flow. The axial flow occurs due to the speed of the fiber along its axis, and the cross flow is due to the air blowing across the fiber. So, the effective heat transfer coefficient, h_t, can be assumed as a sum of two individual contributions [Paek and Schroeder, 1979],

$$h_t = h + h_a, \tag{4.15}$$

where h is the coefficient of heat transfer due to the axial flow as given in Eq. (4.12), and h_a is the heat transfer due to cross flow. h_a can be found as [Paek and Schroeder, 1979],

$$h_a = \frac{k_a}{2a}\left(\frac{T_f}{T_0}\right)^{0.154}\left(0.384 + 0.581R_e^{\,0.439}\right) \quad , \tag{4.16}$$

where k_a is the thermal conductivity of the fluid, T_f is the temperature of the air film surrounding the fiber and R_e is the Reynolds number.

Once h_t is known, the blower length (L) along the axis of the fiber can be found by [Paek and Schroeder, 1979],

$$L = \frac{0.8a\rho C_p}{h_t} V_f. \tag{4.17}$$

Eq. (4.17) indicates that the blower length is directly proportional to the coating speed but inversely proportional to h_t (or equivalently to the air flow velocity).

In a forced cooling system one must insure that the cooling is being applied below the origin (i.e. z=0), otherwise the neck-down shape would be disturbed affecting the fiber diameter control.

b) Pressurized coating applicator: In open cup coating if the speed is higher than a certain limit, the fiber starts to slip, because the adhesion of the coating fluid to the fiber can not be sustained at that high drag force. This slippage is due to the deviation from the Newtonian flow in the coating fluid at a high shear rate [Wagatasuma et al., 1982]. Pressurized coating method can be applied to avoid the slip at high-speed coating. Fig. 4.5 shows the schematic of a

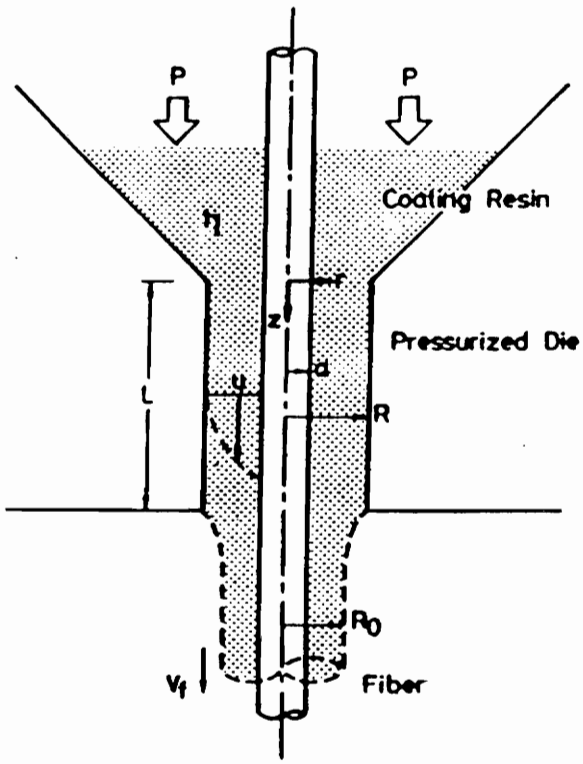

Fig. 4.5 Schematic of a pressurized coating applicator [Sakaguchi et al., 1985].

pressurized coating method. The speed component of the coating fluid along the z axis is designated by u and can be expressed by the equation [Paek and Schroeder, 1979],

$$\frac{\partial^2 u}{\partial r^2} + \frac{1}{r}\frac{\partial u}{\partial r} = \frac{1}{\eta}\frac{\partial P}{\partial z} \quad , \tag{4.18}$$

where η is the viscosity of the coating fluid and P is the pressure as a function of the axial distance z. Eq. (4.18) can be solved under the boundary conditions:

$$\begin{aligned} u &= V_f \qquad at \qquad r = a \ , \\ u &= 0, \qquad at \qquad r = R \ , \end{aligned} \tag{4.19}$$

where $2a$ and $2R$ are the diameters of the fiber and die, respectively. The shear rate in pressurized coating is controlled by applying optimum pressure. The pressure is optimum when the absolute shear rate is the minimum, i.e., when,

$$\frac{\partial u}{\partial r} = 0, \qquad \text{at} \qquad r = a \tag{4.20}$$

The optimum pressure gradient is found by solving Eq. (4.18) under the boundary conditions of Eq. (4.19) and Eq. (4.20) and is found as [Sakaguchi and Kimura, 1985],

$$\frac{\partial P}{\partial z} = \frac{4\eta V_f}{a^2 - R^2 - 2a^2 \ln\frac{a}{R}}. \tag{4.21}$$

Eq. (4.21) gives the optimum conditions for pressurizing the coating fluid. Usually the gradient is represented by $\Delta P/L$, where L is an effective die length. Eq. (4.21) indicates that the optimum pressure is proportional to fiber speed as well as the viscosity of the coating fluid.

c) Draw tension: The draw tension increases with the increase of coating speed, because, the increase of the speed increases the shear rate acting on the fiber. The draw tension (F) of a

fiber can be calculated by integrating the shear stress τ_{rz} acting on the surface that can be written as,

$$\tau_{rz} = \mu\dot{\gamma} \quad , \tag{4.22}$$

where μ is the viscosity of the coating fluid and $\dot{\gamma}$ is the shear rate expressed as [Paek and Schroeder],

$$\dot{\gamma} = \left.\frac{\partial u}{\partial r}\right|_a \tag{4.23}$$

where u is the velocity component of the coating fluid along the z axis of a conical shape applicator, and r is the radial distance measured from the fiber center.

If the conical shape applicator has an inlet diameter of $2R_1$ and an exiting hole size $2R_2$, the total tension acting on the fiber is calculated as [Paek and Schroeder, 1981 (December)],

$$F = \frac{2\pi a\mu KLV_f}{R_1 - R_2}\ln\left(\frac{R_1 - a}{R_2 - a}\right) \quad , \tag{4.24}$$

where K is a constant and L is the die length. Eq. (4.20) shows that there are several ways which can be utilized to decrease the fiber tension, e.g., shorter die length, smaller fiber diameter, lower viscosity of the coating fluid etc. Eq. (4.20) also shows that the tension is directly proportional to coating speed.

Fig. 4.6 shows measured drawing tension with and without coating with the change of coating speed. In the figure the tension increases linearly as the speed increases only up to a certain point and then decreases gradually. The increase of speed generates heating at the interface of fiber and coating fluid and can reduce the viscosity of the fluid resulting a reduced tension.

d) photopolymerization power: The photopolymerization power to cure a particular coating increases linearly with the increase of coating speed, as can be seen from Eq. (4.11). Remember that Eq. (4.11) gives the power absorbed in the coating fluid, not the power produced by the UV lamp. In a real system there are losses involved depending on spectral power conversion of the lamp, efficiency of the reflector and absorptivity of the coating fluid. All these losses must be considered in calculating the required total power output of the UV lamp.

High pressure mercury arc lamps are often used in high-speed cure of coating fluid by photochemical reactions. Only the power which is in a spectral range (usually 300-400 nm) for which the coating fluid has significant absorptivity will be of use in producing the free radicals, while the rest of the power will be wasted. The lamp efficiency (ε_1) can be expressed as the ratio of the power in the effective range to the rated power of the lamp.

The reflector efficiency (ε_2) depends on the shape of the reflector. Fig. 4.7 shows the schematic of a cylindroid reflector, several of which centered around the fiber axis can be used to provide energy to the coating polymer. As shown in Fig. 4.7, the energy radiated within the angle β is diverging and provides little contribution to photopolymerization. Also the radiant flux within the angle δ behind the lamp is blocked by its own body, and can not contribute to the polymerization process at all. Only the rays emanating from an angle range of $[2\pi-(\beta+\delta)]$ are focused by the cylindroid and can contribute significantly in the photochemical reactions. All these factors can be included in reflector efficiency ε_2.

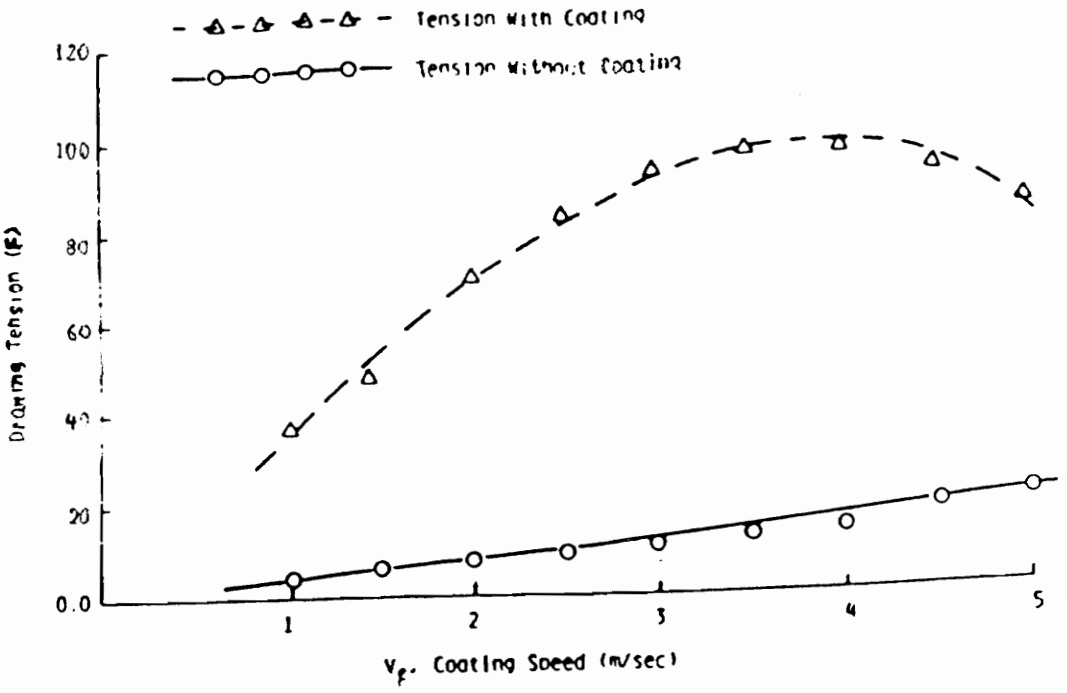

Fig. 4.6 Drawing tension versus coating speed [Paek and Schroeder, 1981 (Dec.)].

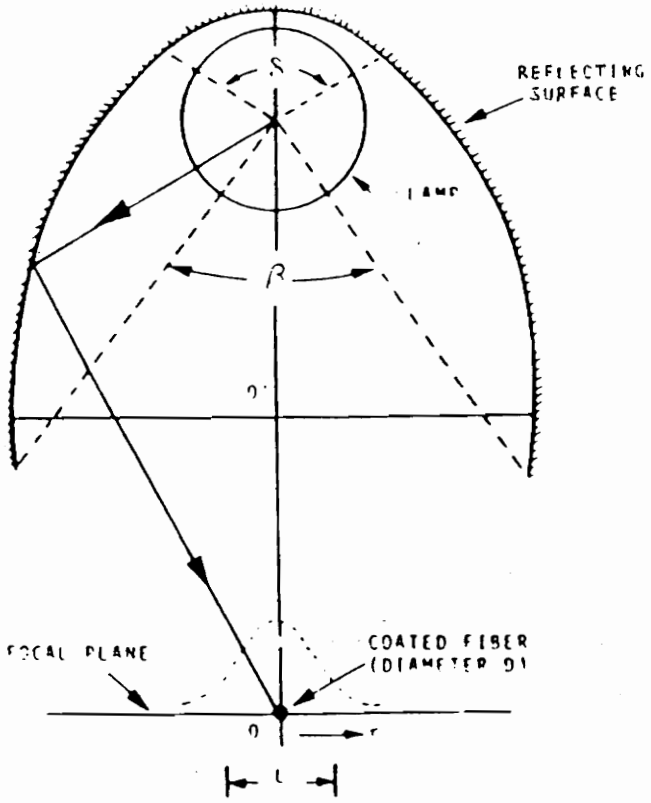

Fig. 4.7 Cylindroid reflector and arc lamp [Paek and Schroeder, 1981(April)].

thickness. The radiation incident on an absorbing substance decreases exponentially when passing through its thickness [Paek and Schroeder, 1981 (April)].

The total efficiency (ε) of the UV system can be given as,

$$\varepsilon = \varepsilon_1 \varepsilon_2 \varepsilon_3 \cdot , \tag{4.25}$$

and the total output power required by the UV lamp can be found from Eq. (4.11) as,

$$P_{total} = \frac{1.6 V_f}{\varepsilon}. \tag{4.26}$$

For a typical high-speed coating system, for example, $\varepsilon_1 = 0.15$, $\varepsilon_2 = 0.01$, $\varepsilon_3 = 0.5$ and $V_f = 10$ m/sec, we get a total power required in excess of 20 KW.

4.6 UV Radiation Induced Losses in Optical Fibers

Intense UV radiation used in crosslinking prepolymer liquids to form coatings around the optical fiber has been observed to induce wavelength dependent transmission losses especially in fibers having germanium or phosphorous doped cores [Blyer et al., 1980]. The losses observed are insignificant for fibers having borosilicate core. It is assumed that UV exposure to germanium or phosphorous doped fibers produces energetic electrons or holes which can become trapped inside the glass network at some defected site and can produce optical absorption bands, or color centers, which increase the attenuation of the fiber. The losses would have been enormous, up to several hundred dB/Km in the near infrared region, if uncoated fibers were given the same level of UV exposure encountered during coating operations.

It has been observed that UV wavelengths less than 300 nm are completely opaque to usual coating fluid thickness and are entirely absorbed by the coating fluid before reaching the fiber core. However, wavelengths greater than 300 nm are quite transparent for typical coating materials and thicknesses. It is therefore essential to limit the penetration of wavelength greater than 300 nm through the coating. Note, however, that limiting the penetration must be done without disturbing the action of the photoinitiator which usually absorbs in the range 300 to 400 nm to produce free radicals which initiate the crosslinking reaction. One way to limit the penetration is to use an external filter to selectively screen UV wavelengths from reaching the coated fiber. Another way is to add selective UV absorber to prepolymer coating fluid so that it can absorb the unwanted wavelengths before reaching the fiber [Blyer et al., 1980].

CHAPTER 5

Conclusion and Suggestions for Future Research

5.1 Conclusion

In this thesis we have shown that an optical fiber must be kept always at the center of the measuring window of the diameter measuring system to measure the on-line fiber diameter accurately. The fiber tends to move easily from the center of the measuring window, due to bends in the preform, nonuniform neck-down shape, or vibrations. We implemented a feedback system to the preform X-Y position, using a PLC, to control the drift of the fiber due to bends in the preform or nonuniform neck-down shape, to insure that the fiber is always at the center of the measuring window. The implemented feedback was discrete in nature, it returns the fiber to the measuring center only when the fiber moves away a predetermined distance from the center, to prevent the introduction of any unwanted vibration of the fiber due to the feedback itself.

In this thesis, we have also developed a procedure to make glass standards for calibration of the on-line fiber diameter measuring systems. Calibrating diameter measuring systems with conventional metallic standards introduce an offset in the measurement of the diameter of glass fiber, the offset can be avoided by using glass standards for the calibration of the diameter measuring systems.

We investigated the overall draw process and found that the shape and behavior of the neck-down region of the melting preform is very important in making the fiber high in tensile strength and uniform in

geometry. The neck-down shape is mainly controlled by the heating profile and temperature of the furnace, the drawing tension of the fiber, the drawing speed of the fiber, and of course the diameter of the preform. As we have seen in Chapter 2, drawing may induce losses in the fiber, especially in germanium and phosphorus doped fibers, the amount of loss depending on the doping concentration. Drawing can also induce residual stress at the core-cladding interface, which may reduce the fiber strength and increase the transmission loss. Coating is very important to protect the fiber and must be applied and cured on-line before any damage can occur on to the fiber surface. The thickness and concentricity of coating mainly depends on the geometric shape of the coating applicator. It is interesting to note that the coating thickness does not depend on drawing speed of the fiber. The modern fiber fabrication processes are heading more and more towards high-speed drawing to reduce the overhead costs and also to improve the fiber performance such as low transmission losses. As a result, high-speed coating is of great importance. Special techniques such as: (a) on-line cooling of the fiber, (b) pressurized coating applicator, (c) high draw tension, and (d) high power UV light source may be applied for high-speed coating.

5.2 Suggestions for Future Research

In drawing fiber from a glass preform, one of the most challenging jobs is to determine the optimum drawing condition and to maintain that condition throughout the draw process. The interrelations among furnace temperature, draw speed, tension, optical loss and strength of the fiber are still not properly realized. Relations have been found in the literature which oppose each other [Imoto et al., 1978] [Oh et al., 1983][DiMarcello et al., 1985]. Further research in this area is required to establish a better understanding of these relationships.

In measuring on-line fiber diameter, the vibration of the fiber poses a real threat to increasing the level of measurement accuracy. In the scanning beam diameter measuring technique, the scanning rate of the laser is usually at a range of 1 KHz. If the vibrating frequencies of the fiber is comparable to 1 KHz, the accuracy of the measurement can not be maintained. Preform vibrations during the drawing process are unavoidable, but attempts may be made to reduce the amplitude of these vibrations. Until now, as far as we know, no research has been conducted in this area. Knowledge of resonant frequencies of vibration, amplitudes of vibration and the minimum required scanning rate of the laser for a particular type of vibration is essential to improve the fiber diameter measuring accuracy.

APPENDIX

The Series 90-30 PLC is a product of GE Fanuc. It offers advanced programming features and provides easier system integration. Fig.1 shows a GE Fanuc Series 90-30 PLC with *Model 311 CPU*. The PLC can include the following components:

- 5-slot CPU Baseplate
- 30 watt power supply (120/240 VAC or 125 VDC, and 24/48 VDC input)
- Discrete Input and Output modules
- Analog Input and Analog Output modules
- Programmable Coprocessor modules
- Alphanumeric Display Coprocessor module
- Communications Control module
- High-Speed Counter module
- I/O Link Interface module
- Axis Positioning module
- Hand-Held Programmer
- State Logic Processor module

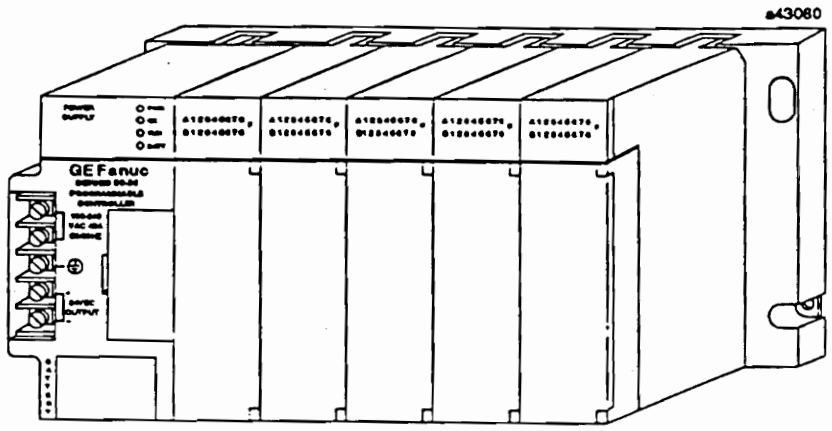

Fig. A GE Fanuc Series 90-30 PLC with Model 311 CPU [GE Fanuc Automation, 1993].

GE Fanuc Series 90-30 PLC can be programmed as well as configured by using Logicmaster 90 programming software [GE Fanuc Automation, 1990]. Logicmaster 90 uses ladder logic to control the PLC. The ladder logic program developed to control the X-Y position of the fiber inside the window of the Dia Measuring System is given below.

rev 1.6 August 13,1993

```
 GGGG EEEEE        FFFFF  AAA  N   N U   U  CCCC
G     E            F     A   A NN  N U   U C
G GGG EEEE         FFF   AAAAA N N N U   U C
G   G E            F     A   A N  NN U   U C
 GGG  EEEEE        F     A   A N   N  UUU   CCCC


 AAA  U   U TTTTT  OOO  M   M  AAA  TTTTT IIIII  OOO  N   N
A   A U   U   T   O   O MM MM A   A   T     I   O   O NN  N
AAAAA U   U   T   O   O M M M AAAAA   T     I   O   O N N N
A   A U   U   T   O   O M   M A   A   T     I   O   O N  NN
A   A  UUU    T    OOO  M   M A   A   T   IIIII  OOO  N   N
```

```
(*****************************************************************************)
(                                                                             )
(      CENTRAL PLC CONFIGURATION                                              )
(                                                                             )
(                                                                             )
(              TOTAL DISCRETE I/O (%I + %Q):      72                        )
(                                                                             )
(              HIGHEST CONFIGURED REFERENCES                                  )
(              -----------------------------                                  )
(              DISCRETE INPUT          (%I) :     48                        )
(              DISCRETE OUTPUT         (%Q) :     48                        )
(                                                                             )
(              ANALOG INPUT           (%AI) :     47                        )
(              ANALOG OUTPUT          (%AQ) :      0                        )
(                                                                             )
(              REGISTER MEMORY         (%R) :      0                        )
(                                                                             )
(*****************************************************************************)
```

Folder: C:\LM90\XYCONT

			RACK 0		
PS/CPU	1	2	3	4	5
	PROGRAMMED		CONFIGURATION		
PWR321	MDL654	ALG220	APU300	MDL930	
CPU 30	I DC32	IALGV4	HSC	Q RLY8	
	RefAdr %I0001	RefAdr %AI0001	RefAdr %QI0033 %AI0033	RefAdr %Q0001	

```
        SERIES 90-30 MODULE IN RACK 0 SLOT  0
+------+------------------ SOFTWARE  CONFIGURATION ----------------------------
| SLOT |  Catalog #: IC693PWR321            POWER SUPPLY 120/240 VAC 30 W
|   0  |
|PWR321|-------------------------------------------------------------------------
| CPU 30|
|      |
|      |
|      |
|      |
|      |
|      |
+------+
```

```
        SERIES 90-30 MODULE IN RACK 0 SLOT  0
+------+------------------ SOFTWARE  CONFIGURATION ----------------------------
| SLOT |  Catalog #: IC693CPU311            BASE 5-SLOT WITH CPU 311
|   0  |
|      |
|CPU311|-------------------------------------------------------------------------
|      |  IOScan-Stop: NO        Baud Rate  : 19200
|8 MHZ |  Pwr Up Mode: LAST      Parity     : ODD
|      |  Logic From : RAM       Stop Bits  : 1
|      |  Registers  : RAM       Modem TT   :   0       1/100 Second / Count
|      |  Passwords  : ENABLED   Idle Time  :  10       Seconds
|      |
|      |
|      |  Chksum Wrds:   8       Sweep Mode : NORMAL
|      |                         Sweep Tmr  : N/A       msec
|      |
+------+
```

SERIES 90-30 MODULE IN RACK 0 SLOT 1

SLOT	SOFTWARE CONFIGURATION	
1	Catalog #: IC693MDL654	INPUT 5/12 VDC 32PT POS/NEG
	Ref Addr : %I0001	Size : 32
MDL654		
I DC32		
RefAdr %I0001		

SERIES 90-30 MODULE IN RACK 0 SLOT 2

SLOT	SOFTWARE CONFIGURATION	
2	Catalog #: IC693ALG220	INPUT ANALOG 4PT VOLTAGE
	Ref Addr : %AI0001	Size : 4
ALG220		
IALGV4		
RefAdr AI0001		

```
        SERIES 90-30 MODULE IN RACK 0 SLOT  3
+-------+------------------ SOFTWARE  CONFIGURATION ----------------------------
| SLOT  |  Catalog #: IC693APU300             HIGH SPEED COUNTER MODULE
|   3   |
|       |
|APU300 |-------------------------------------------------------------------------
|       |  Counter Typ: B          Cnt Filt 1 : HIFREQ
|HSC    |  Ctrl/Status:  %QI0033   Cnt Filt 2 : HIFREQ
|       |  HSC Data   :  %AI0033   Pld Filt1&2: HIFREQ
|       |  Failure Mde: HOLDLAST   Disbl Filt1: HIFREQ
|       |  Osc Input  : OFF        Disbl Filt2: HIFREQ
|       |  Osc Divider:   660
|       |
|       |
|       |
|       |
+-------+
```

```
        SERIES 90-30 MODULE IN RACK 0 SLOT  3
+-------+------------------ SOFTWARE  CONFIGURATION ----------------------------
| SLOT  |  Catalog #: IC693APU300             HIGH SPEED COUNTER MODULE
|   3   |
|       |
|APU300 |-------------------------------------------------------------------------
|       |                ----------      TYPE  B   COUNTER  1   ----------
|HSC    |  Count Mode :  SINGSHOT                  On Preset 1:  +0008388607
|       |  Cnt Sig    :  AQUADB                    Off Preset1:  +0000000000
|       |  Time Base  :   1000                     On Preset 2:  +0008388607
|       |  Strobe1 Edg:  POS                       Off Preset2:  +0000000000
|       |  Strobe2 Edg:  POS
|       |  Hi Limit   :  +0000999999
|       |  Lo Limit   :  -0000010000
|       |  Pld Value  :  +0000000000
|       |
+-------+
```

Folder: C:\LM90\XYCONT Slot

SERIES 90-30 MODULE IN RACK 0 SLOT 3

SLOT	SOFTWARE CONFIGURATION			
3	Catalog #: IC693APU300		HIGH SPEED COUNTER MODULE	
APU300				
	----------	TYPE B	COUNTER 2	----------
HSC	Count Mode : CONTINU		On Preset 1:	+0008388607
	Cnt Sig : PULS/DIR		Off Preset1:	+0000000000
	Time Base : 1000		On Preset 2:	+0008388607
	Strobe1 Edg: POS		Off Preset2:	+0000000000
	Strobe2 Edg: POS			
	Hi Limit : +0008388607			
	Lo Limit : +0000000000			
	Pld Value : +0000000000			

SERIES 90-30 MODULE IN RACK 0 SLOT 4

SLOT	SOFTWARE CONFIGURATION		
4	Catalog #: IC693MDL930	OUTPUT RELAY 4A 8PT ISOLATED	
	Ref Addr : %Q0001	Size : 8	
MDL930			
Q RLY8			
RefAdr %Q0001			

Folder: C:\LM90\XYCONT Slot

rev 1.6 August 13,1993

DISCRETE INPUTS (%I)

TOTAL I+Q: 72

HIGHEST REF CONFIGURED: 48

REFERENCE START - END	PHYSICAL ADDRESS	IO TYPE	MODULE TYPE	DESCRIPTION
00001-00032	0.1	90-30	I DC12	INPUT 5/12 VDC 32PT POS/NEG
00033-00048	0.3	90-30	HSC	HIGH SPEED COUNTER MODULE

DISCRETE OUTPUTS (%Q)

TOTAL I+Q: 72 HIGHEST REF CONFIGURED: 48.

REFERENCE START - END	PHYSICAL ADDRESS	IO TYPE	MODULE TYPE	DESCRIPTION
00001-00008	0.4	90-30	Q RLY8	OUTPUT RELAY 4A 8PT ISOLATED
00033-00048	0.3	90-30	HSC	HIGH SPEED COUNTER MODULE

rev 1.6 August 13,1993

ANALOG INPUTS (%AI)

TOTAL USED: 19 HIGHEST REF CONFIGURED: 47

REFERENCE START - END	PHYSICAL ADDRESS	IO TYPE	MODULE TYPE	DESCRIPTION
00001-00004	0.2	90-30	IALGV4	INPUT ANALOG 4PT VOLTAGE
00033-00047	0.3	90-30	HSC	HIGH SPEED COUNTER MODULE

CPU MEMORY CONFIGURATION FOR Model 311 CPU:

Discrete Input	(%I)	512	Points
Discrete Output	(%Q)	512	Points
Internal Discrete	(%M)	1024	Points
System Use	(%S)	128	Points
Temporary Status	(%T)	256	Points
GENIUS Global	(%G)	1280	Points
TOTAL DISCRETE MEMORY:		3712	Points
Analog Input	(%AI)	64	Words
Analog Output	(%AQ)	32	Words
Register Memory	(%R)	512	Words
TOTAL LOGIC MEMORY		4928	Bytes
CPU MEMORY TOTAL		6144	Bytes

POINT FAULT REFERENCE DISABLED

FAULT CATEGORY CONFIGURATION:

Loss of or Missing Rack	F
Loss of or Missing IOC	F
Loss of or Missing I/O Module	F
Loss of or Missing Option Module	F
System Bus Failure	F
IOC Fault (I/O Bus Fault)	F
System Config Mismatch	F

```
[  START OF LD  PROGRAM XYCONT   ]       (* X-Y/SSC PROGRAM KEE 7-12-93 0.0  *)

[     VARIABLE DECLARATIONS      ]

[       BLOCK DECLARATIONS       ]

[     START OF PROGRAM LOGIC     ]

 (*****************************************************************************)
 (* X-Y POSITION CONTROL LOGIC                                                *)
 (*                                                                           *)
 (*****************************************************************************)

 << RUNG 5  STEP #0002 >>

ALW_ON
%S0007  +------+
+--] [---+MOVE_+-
         | INT  |
         |      |
         |      | TRIGGER
 CONST --+IN  Q+-%R0001
 +00001  | LEN  |
         |00001 |
         |      |
         +------+

 << RUNG 6  STEP #0004 >>

SETS     DEFEATS                                                    INTERNA
AUTO     HOLDING                                                    L RELAY
X-Y      OF AUTO                                                    OPERATI
CONTROL  SWITCH                                                     ON
AUTOXY   NOTAUTO                                                    AUTOSET
%I0003   %Q0101                                                     %Q0100
+--] [-----]/[-------------------------------------------------------(S)--

 << RUNG 7  STEP #0007 >>

INTERNA                                                             AUTO
L RELAY                                                             X-Y
OPERATI                                                             CONTROL
ON                                                                  LAMP
AUTOSET                                                             AXYLAMP
%Q0100                                                              %Q0008
+--] [--------------------------------------------------------------( )--

REFERENCE NICKNAME      REFERENCE DESCRIPTION
 %S0007   ALW_ON
 %Q0100   AUTOSET       INTERNAL RELAY OPERATION
 %I0003   AUTOXY        SETS AUTO X-Y CONTROL
 %Q0008   AXYLAMP       AUTO X-Y CONTROL LAMP
 %Q0101   NOTAUTO       DEFEATS HOLDING OF AUTO SWITCH
 %R0001   TRIGGER

Program: XYCONT                C:\LM90\XYCONT                Block: _MAIN
```

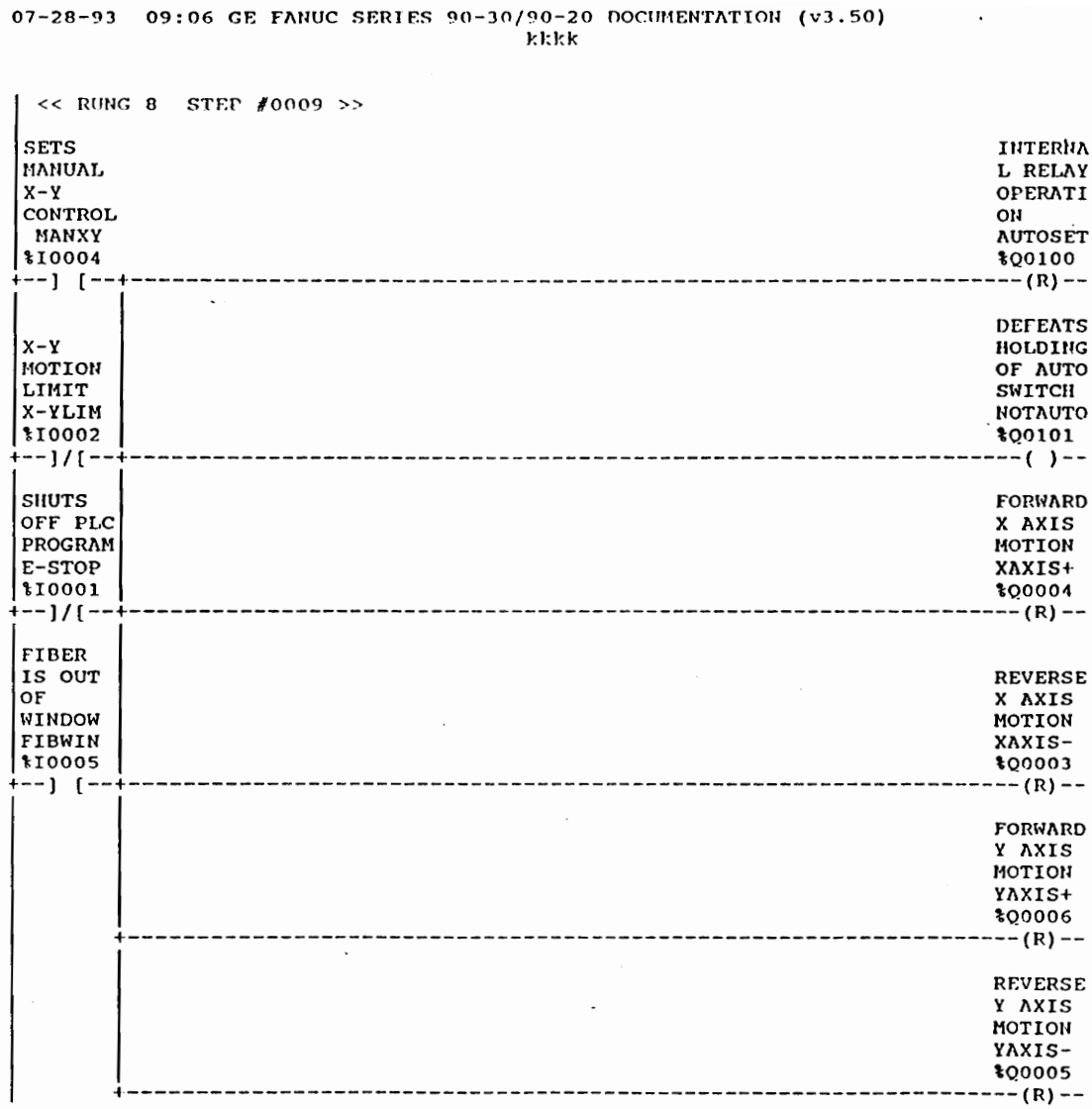

REFERENCE	NICKNAME	REFERENCE DESCRIPTION
%Q0100	AUTOSET	INTERNAL RELAY OPERATION
%I0001	E-STOP	SHUTS OFF PLC PROGRAM
%I0005	FIBWIN	FIBER IS OUT OF WINDOW
%I0004	MANXY	SETS MANUAL X-Y CONTROL
%Q0101	NOTAUTO	DEFEATS HOLDING OF AUTO SWITCH
%I0002	X-YLIM	X-Y MOTION LIMIT

Program: XYCONT C:\LM90\XYCONT Block: _MAIN

REFERENCE	NICKNAME	REFERENCE DESCRIPTION
%Q0004	XAXIS+	FORWARD X AXIS MOTION
%Q0003	XAXIS-	REVERSE X AXIS MOTION
%Q0006	YAXIS+	FORWARD Y AXIS MOTION
%Q0005	YAXIS-	REVERSE Y AXIS MOTION

```
 << RUNG 9  STEP #0019 >>

DEFEATS
HOLDING
OF AUTO
SWITCH
NOTAUTO                                                                MSGRST
%Q0101  +-----+                                                        %M0001
+--] [---+MOVE_+------------------------------------------------------------( )--
         | INT |
         |     |
         |     | TRIGGER
 CONST -+IN  Q+-%R0001
 +00003 | LEN |
        |00001|
        |     |
        +-----+

 << RUNG 10  STEP #0022 >>

                                                                       FUTURE
                                                                       CUT
                                                                       ALERT
                                                                       OUTPUT
MSGRST                                                                 CUTWARN
%M0001  +-----+                                                        %Q0002
+--] [---+MOVE_+------------------------------------------------------------( )--
         | INT |
         |     |
         |     | TRIGGER
 CONST -+IN  Q+-%R0001
 +00000 | LEN |
        |00001|
        |     |
        +-----+
```

REFERENCE	NICKNAME	REFERENCE DESCRIPTION
%Q0002	CUTWARN	FUTURE CUT ALERT OUTPUT
%M0001	MSGRST	
%Q0101	NOTAUTO	DEFEATS HOLDING OF AUTO SWITCH
%R0001	TRIGGER	

Program: XYCONT C:\LM90\XYCONT Block: _MAIN

```
 << RUNG 11  STEP #0025 >>

INTERNA
L RELAY                                                              FORWARD
OPERATI                                                              X AXIS
ON                                                                   MOTION
AUTOSET                                                              XAXIS+
%Q0100  +-----+                                                      %Q0004
+--] [---+ LT  |+-----------------------------------------------------(S)--
         | INT ||
         |     ||
ANALOG   |     ||
VALUE O  |     ||
F X AXI  |     ||
S POSIT  |     ||
XAXPOS   |     ||
%AI001 -+I1  Q++|
         |     |
 CONST -+I2    |
 +00000 +-----+

 << RUNG 12  STEP #0028 >>

INTERNA
L RELAY                                                              FORWARD
OPERATI                                                              X AXIS
ON                                                                   MOTION
AUTOSET                                                              XAXIS+
%Q0100  +-----+                                                      %Q0004
+--] [---+ GE  |+-----------------------------------------------------(R)--
         | INT ||
         |     ||
ANALOG   |     ||
VALUE O  |     ||
F X AXI  |     ||
S POSIT  |     ||
XAXPOS   |     ||
%AI001 -+I1  Q++|
         |     |
 CONST -+I2    |
 +00000 +-----+
```

REFERENCE	NICKNAME	REFERENCE DESCRIPTION
%Q0100	AUTOSET	INTERNAL RELAY OPERATION
%Q0004	XAXIS+	FORWARD X AXIS MOTION
%AI001	XAXPOS	ANALOG VALUE OF X AXIS POSITION

Program: XYCONT C:\LM90\XYCONT Block: _MAIN

```
 << RUNG 13  STEP #0031 >>

INTERNA
L RELAY                                                          REVERSE
OPERATI                                                          X AXIS
ON                                                               MOTION
AUTOSET                                                          XAXIS-
%Q0100  +-----+                                                  %Q0003
+--] [---+ GT_ |+-----------------------------------------------------(S)--
         | INT ||
ANALOG   |     ||
VALUE O  |     ||
F X AXI  |     ||
S POSIT  |     ||
XAXPOS   |     ||
%AI001 -+I1  Q++
         |     |
 CONST -+I2    |
 +00000 +-----+

 << RUNG 14  STEP #0034 >>

INTERNA
L RELAY                                                          REVERSE
OPERATI                                                          X AXIS
ON                                                               MOTION
AUTOSET                                                          XAXIS-
%Q0100  +-----+                                                  %Q0003
+--] [---+ LE_ |+-----------------------------------------------------(R)--
         | INT ||
ANALOG   |     ||
VALUE O  |     ||
F X AXI  |     ||
S POSIT  |     ||
XAXPOS   |     ||
%AI001 -+I1  Q++
         |     |
 CONST -+I2    |
 +00000 +-----+
```

REFERENCE	NICKNAME	REFERENCE DESCRIPTION
%Q0100	AUTOSET	INTERNAL RELAY OPERATION
%Q0003	XAXIS-	REVERSE X AXIS MOTION
%AI001	XAXPOS	ANALOG VALUE OF X AXIS POSITION

Program: XYCONT C:\LM90\XYCONT Block: _MAIN

```
 << RUNG 15  STEP #0037 >>

INTERNA
L RELAY                                                              FORWARD
OPERATI                                                              Y AXIS
ON                                                                   MOTION
AUTOSET                                                              YAXIS+
%Q0100  +-----+                                                      %Q0006
+--] [---+ LT_  |+-----------------------------------------------------(S)--
         | INT  ||
         |      ||
ANALOG   |      ||
VALUE O  |      ||
F Y AXI  |      ||
S POSIT  |      ||
YAXPOS   |      ||
%AI002 -+I1  Q++
         |      |
 CONST -+I2     |
 +00000 +-----+

 << RUNG 16  STEP #0040 >>

INTERNA
L RELAY                                                              FORWARD
OPERATI                                                              Y AXIS
ON                                                                   MOTION
AUTOSET                                                              YAXIS+
%Q0100  +-----+                                                      %Q0006
+--] [---+ GE_  |+-----------------------------------------------------(R)--
         | INT  ||
         |      ||
ANALOG   |      ||
VALUE O  |      ||
F Y AXI  |      ||
S POSIT  |      ||
YAXPOS   |      ||
%AI002 -+I1  Q++
         |      |
 CONST -+I2     |
 +00000 +-----+
```

REFERENCE	NICKNAME	REFERENCE DESCRIPTION
%Q0100	AUTOSET	INTERNAL RELAY OPERATION
%Q0006	YAXIS+	FORWARD Y AXIS MOTION
%AI002	YAXPOS	ANALOG VALUE OF Y AXIS POSITION

Program: XYCONT C:\LM90\XYCONT Block: _MAIN

```
 << RUNG 17  STEP #0043 >>

INTERNA
L RELAY                                                              REVERSE
OPERATI                                                              Y AXIS
ON                                                                   MOTION
AUTOSET                                                              YAXIS-
%Q0100  +-----+                                                      %Q0005
+--] [---+ GT  |+-----------------------------------------------------(S)--
         | INT ||
         |     ||
ANALOG   |     ||
VALUE O  |     ||
F Y AXI  |     ||
S POSIT  |     ||
YAXPOS   |     ||
%AI002 -+I1  Q++
         |     |
 CONST -+I2    |
 +00000 +-----+

 << RUNG 18  STEP #0046 >>

INTERNA
L RELAY                                                              REVERSE
OPERATI                                                              Y AXIS
ON                                                                   MOTION
AUTOSET                                                              YAXIS-
%Q0100  +-----+                                                      %Q0005
+--] [---+ LE  |+-----------------------------------------------------(R)--
         | INT ||
         |     ||
ANALOG   |     ||
VALUE O  |     ||
F Y AXI  |     ||
S POSIT  |     ||
YAXPOS   |     ||
%AI002 -+I1  Q++
         |     |
 CONST -+I2    |
 +00000 +-----+

 (*************************************************************************)
 (* window boundaries                                                     *)
 (*                                                                       *)
 (*************************************************************************)
```

REFERENCE	NICKNAME	REFERENCE DESCRIPTION
%Q0100	AUTOSET	INTERNAL RELAY OPERATION
%Q0005	YAXIS-	REVERSE Y AXIS MOTION
%AI002	YAXPOS	ANALOG VALUE OF Y AXIS POSITION

Program: XYCONT C:\LM90\XYCONT Block: _MAIN

```
 << RUNG 20  STEP #0050 >>

INTERNA
L RELAY
OPERATI
ON
AUTOSET                                                              OR1
%Q0100  +-----+                                                    %Q0102
+--] [---+ GE_  |+-------------------------------------------------------( )--
         | INT  ||
                ||
ANALOG          ||
VALUE O         ||
F X AXI         ||
S POSIT         ||
XAXPOS          ||
%AI001 -+I1  Q++
        |
 CONST -+I2   |
 +25600 +-----+

 << RUNG 21  STEP #0053 >>

INTERNA
L RELAY
OPERATI
ON
AUTOSET                                                              OR2
%Q0100  +-----+                                                    %Q0103
+--] [---+ LE_  |+-------------------------------------------------------( )--
         | INT  ||
                ||
ANALOG          ||
VALUE O         ||
F X AXI         ||
S POSIT         ||
XAXPOS          ||
%AI001 -+I1  Q++
        |
 CONST -+I2   |
 -25600 +-----+
```

REFERENCE	NICKNAME	REFERENCE DESCRIPTION
%Q0100	AUTOSET	INTERNAL RELAY OPERATION
%Q0102	OR1	
%Q0103	OR2	
%AI001	XAXPOS	ANALOG VALUE OF X AXIS POSITION

Program: XYCONT C:\LM90\XYCONT Block: _MAIN

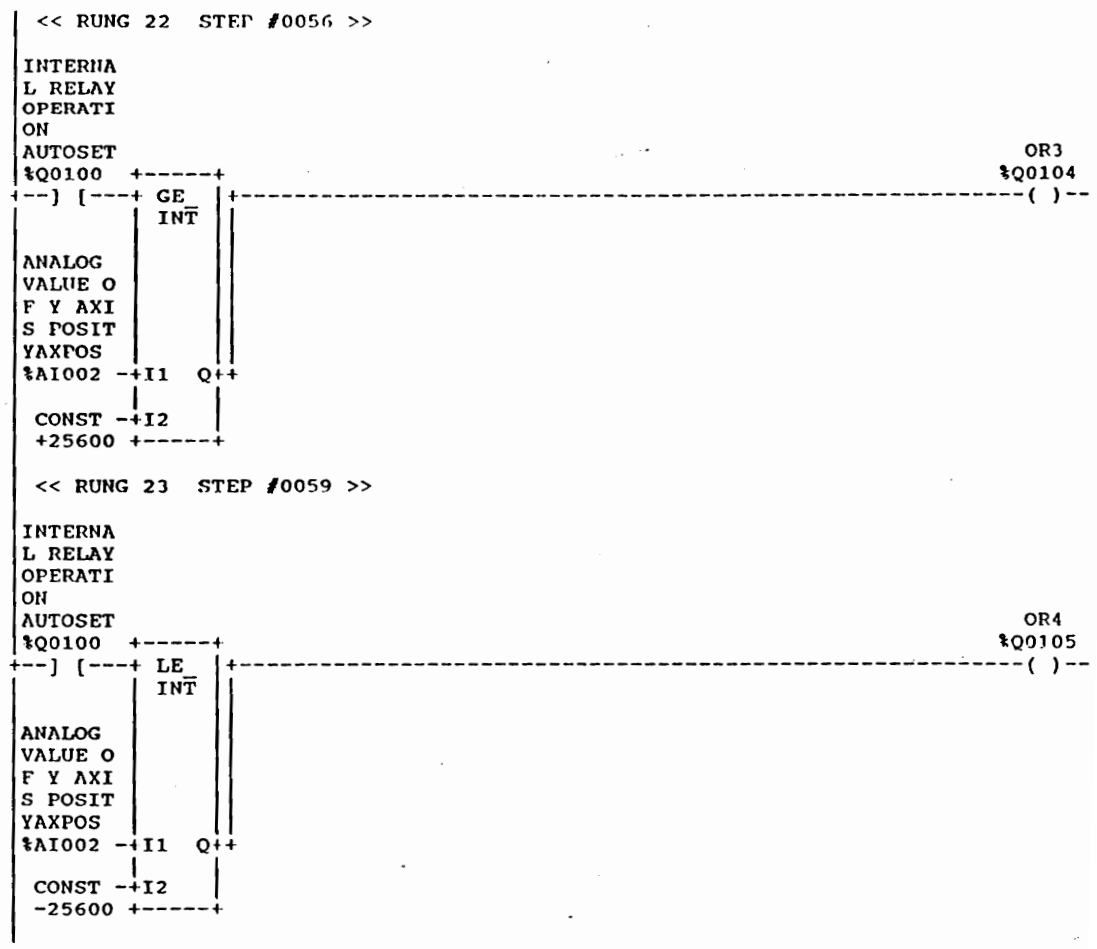

REFERENCE	NICKNAME	REFERENCE DESCRIPTION
%Q0100	AUTOSET	INTERNAL RELAY OPERATION
%Q0104	OR3	
%Q0105	OR4	
%AI002	YAXPOS	ANALOG VALUE OF Y AXIS POSITION

Program: XYCONT C:\LM90\XYCONT Block: _MAIN

```
|  << RUNG 24  STEP #0062 >>
|
|                                                                          FIBER
|                                                                          CUT
|                                                                          OUTPUT
|   OR1                                                                      CUT
|  %Q0102                                                                  %Q0001
+--] [--+-------------------------------------------------------------------( )--
|       |
|   OR2 |
|  %Q0103
+--] [--+
|       |
|   OR3 |
|  %Q0104
+--] [--+
|       |
|   OR4 |
|  %Q0105
+--] [--+
|       |
| FIBER |
| IS OUT
| OF    |
| WINDOW
| FIBWIN
| %I0005
+--] [--+
|
|  (*************************************************************************)
|  (* SSC PROGRAM LOGIC                                                     *)
|  (*                                                                       *)
|  (*************************************************************************)
|
```

```
REFERENCE NICKNAME      REFERENCE DESCRIPTION
 %Q0001   CUT           FIBER CUT OUTPUT
 %I0005   FIBWIN        FIBER IS OUT OF WINDOW
 %Q0102   OR1
 %Q0103   OR2
 %Q0104   OR3
 %Q0105   OR4

Program: XYCONT                C:\LM90\XYCONT                Block: _MAIN
```

REFERENCES:

Ainslie, B. J., Beales, K. J., Day, C. R., and Rush, J. D."Interplay of design parameters and fabrication conditions on the performance of monomode fibers made by MCVD," *IEEE J. Quantum Electronics*, QE-17, pp 854-857, June 1981.

Anritsu, *Instruction Manual*: M551A/B SLB Dia Measuring System, Anritsu Corp., Tokyo, Japan, 1984, V3.

Baines, J. G. N., Hallam, A. G., Raine, K. W., and Turner, N. P."Fiber diameter measurements and their calibration," *J. Lightwave Tech.*, Vol. LT-8, pp 1259-1268, Sep. 1990.

Blyers, Jr., L. L., and DiMarcello, F.V.,"Fiber Drawing, coating, and jacketing" *Proceedings IEEE*, Vol. 68, pp 1194-1198, Oct. 1980.

Blyers, Jr., L. L., DiMarcello, F. V., Simpson, J. R., Sigety, E. A., Hart, Jr., A. C., Foertmeyer, V. A."UV-radiation induced losses in optical fibers and their control"*J. Non-Cryst. Solids*, Vol. 38-39, pp 165-170, 1980.

Brehm, C., Dupont, P., Lavanant, G., Ledoux, P., Le Sergent, C."Improved drawing conditions for very low loss 1.55 μm dispersion-shifted fiber," *Fiber and Integrated Optics*, Vol. 7, pp 333-341, 1988.

Chida, K., Sakaguchi, S., Wagatsuma, M., Kimura, T."*Electronics Letters*, Vol. 18, pp 713-715, Aug. 1982.

Chu, P. L., Whitbread, T., and Allen, P. M."An on-line fiber drawing tension and diameter measurement device," *J. Lightwave Tech.*, Vol. LT-4, pp 1048-1060, Feb. 1989.

Cocito, G., Roba, G., and Vergnano, P., *In "Optical Fiber Communication"* (edited by Technical Staff of Centro Studi e Laboratori Telecommunicazioni, Torino, Italy), Chap. 4, McGraw-Hill (1981).

Dakin, J., and Culshaw, B. *"Optical fiber sensors: principles and components,"* Artech House, 1988.

DiMarcello, F. V., Kurkjian, C. R., and Williams J. C. *In "Optical Fiber Communications"* (Volume 1, Fiber Fabrication, edited by Tingye Li), Chap 4, Academic Press (1985).

France, P. W., Dunn, P. L., and Reeve, M. H."Plastic coating of glass fibers and its influence on strength," *Fiber and Integrated Optics*, Vol. 2, pp 267-286, 1979.

Gardner, W. B.,"Microbending loss in optical fibers" *Bell Sys. Tech. J.*, Vol. 54, pp 457-465, Feb. 1975.

GE Fanuc Automation, *Installation Manual*: Series 90-30 Programable Controller, GE Fanuc Automation, May 1993.

GE Fanuc Automation, *User's Manual*: Logicmaster 90-30 Programming Software, GE Fanuc Automation, Nov. 1990.

Geyling, F. T., and Homsy, G. M."Extensional instabilities of the glass fibre drawing," *Glass Technology*, Vol. 21, pp 95-102, April 1980.

Homsy, G. M., and Walker, K."Heat transfer in laser drawing of optical fibres," *Glass Technology*, Vol. 20, pp 20-26, Feb. 1979.

Imoto, K., Aoki, S., Sumi, M."Novel method of diameter control in optical fiber drawing process," *Electronics Letters*, Vol. 13, pp 726-727, Nov. 1977.

Imoto, K., Sumi, M."Optical-fibre loss for high-speed drawing," *Electronics Letters*, Vol. 14, pp 749-750, Nov. 1978.

Jeager, R. E., Pearson, A. D., Williams J. C., Presby, H. M. *In "Optical Fiber Telecommunications"* (S. E. Miller and A. G. Chynoweth, editor), Chap. 9, Academic Press (1979).

Kaiser, P."Drawing-induced coloration in vitreous silica fibers" *J. Opt. Soc. Am.*, Vol. 64, pp 475-481, April 1974.

Keiser, G."*Optical Fiber Communications*," 2nd edition, McGraw-Hill, 1991.

Marcuse, D."*Theory of dielectric optical waveguides*," Academic press, 1974.

Montierth, M. R."Recent advances in the production of multimode optical fibers," J. Electronics Materials, Vol. 6, pp 349-372, 1977.

Oehrle, R. C."Galvanometer beam-scanning system for laser fiber drawing," *Applied Optics*, Vol. 18, pp 496-500, 1979.

Oh, S. M."Cooling rate of optical fibers during drawing," *Amer. Ceram. Soc. Bull.*, Vol. 58, pp 1108-1110, 1979.

Oh, P. S., McAlarney, J. J., and Nath K. D."Effect of fiber drawing tension on optical and mechanical properties of optical fiber waveguides," *J. Am. Ceram. Soc.*, Vol. 66, c84-85, May 1983.

Paek, U. C."High-speed high-strength fiber drawing," *J. Lightwave Tech.*, Vol. LT-4, pp 1048-1060, Aug. 1986.

Paek, U. C., and Runk, R. B."Physical behaviors of the neck-down region during furnace drawing of silica fibers," *J. Appl. Phys.*, Vol. 49, pp 4417-4422, Aug. 1978.

Paek, U. C., and Schroeder, C. M."Coating of optical fibers with a conical shape applicator," *Fiber and Integrated Optics*, Vol. 2, pp 287-298, 1979.

Paek, U. C., and Schroeder, C. M."Forced convective cooling of optical fibers in high-speed coating," *J. Appl. Phys.*, Vol. 50, pp 6144-6148, Oct. 1979.

Paek, U. C., and Schroeder, C. M."Calculation of photopolymerization energy required for optical fiber coating," *Applied Optics*, Vol. 20, pp 1230-1233, April 1981.

Paek, U. C., and Schroeder, C. M."High speed coating of optical fibers with UV curable materials at a rate of greater than 5 m/sec," *Applied Optics*, Vol. 20, pp 4028-4034, Dec. 1981.

Presby, H. M."Geometrical uniformity of plastic coatings on optical fibers," *Bell Syst. Tech. J.*, Vol. 55, pp 1525-1537, Dec. 1976.

Sakaguchi, S., and Kimura, T."High-speed drawing of optical fibers with pressurized coatings," *J. Lightwave Tech.*, Vol. LT-3, pp 669-673, June 1985.

Smithgall, D. H., Watkins, L.S., and Frazee, Jr., R. E."High-speed non contact fiber-diameter measurement using forward light scattering," *Applied Optics*, Vol. 16, pp 2395-2402, Sep. 1977.

Wagatsuma, M., Kimura, T., Shuto, Y., and Yamakawa, S."Optical fibre coating speed prediction from flow properties of coating materials," *Electronics Letters*, Vol. 18, pp 731-732, Aug. 1982.

Walker, P., Webers, V. J., Thomas, G. A."Photopolymerizable reproduction system-chemistry and application," *J. Photogr. Sci.*, Vol. 18, pp 150, 1970.

Yamauchi, R., Kobayashi, T., and Inada, K."Coloration and its reduction in phosphorus-doped low-loss optical fibres," *Electronics Letters*, Vol. 13, pp 461-462, Aug. 1977.

VITA

Shah Mohammed Musa was born on August 7, 1966 in Barisal, Bangladesh. Upon graduation from Barisal Zilla School, he attented Brojomohan College, Barisal and then Bangladesh University of Engineering and Technology (BUET), Dhaka. He earned his Bachelor of Science degree in Electrical Engineering in 1991 from BUET and before coming to Virginia Polytechnic Institute and State University as a graduate student, he worked as a teacher in Onnesha International School, Dhaka. During the summer of 1993 he worked with Alcatel Telecommunications, Roanoke on improving the diameter control in optical fiber fabrication. He was a Teaching Assistant to the Department of Electrical Engineering of Virginia Tech for Fall 1993. He is currently a Ph D student in Virginia Tech and is a student member of the Institute of Electrical and Electronics Engineers. He is also a member of Greenpeace, USA.

Shah Musa